TALLINN UNIVERSITY OF TECHNOLOGY
SCHOOL OF ENGINEERING
Department of Materials and Environmental Technology

DEVELOPMENT OF SOLAR PANELS FOR MARINE APPLICATIONS

PÄIKESEPANEELIDE ARENDUS MERERAKENDUSTEKS

MASTER THESIS

Student:	Kaur Ots
Student code:	185009KAYM
Supervisor:	Arvo Mere, Associate Professor
Co-supervisor:	Ander Pukk, Director of Naps Solar Estonia OÜ

Tallinn, 2020

AUTHOR'S DECLARATION

Hereby I declare, that I have written this thesis independently.
No academic degree has been applied for based on this material. All works, major viewpoints and data of the other authors used in this thesis have been referenced.

".....” ..... 20…..

Author: .....
/signature /

Thesis is in accordance with terms and requirements

".....” ..... 20….

Supervisor: ….....
/signature/

Accepted for defence

".....”.....20… .

Chairman of theses defence commission: .....
/name and signature/

THESIS TASK

Student: Kaur Ots, 185009KAYM

Study programme, KAYM, Materials and Processes of Sustainable Energetics

main speciality: Processes of Sustainable energetics

Supervisor: Associate Professor, Arvo Mere, +372 620 3001.

Co-supervisor: Director of Naps Solar Estonia OÜ, Ander Pukk, +372 656 6829

Thesis topic:

(in English) Development of solar panels for marine applications

(in Estonian) Päikesepaneelide arendus mererakendusteks

Thesis main objectives:

1. Explain advantages and disadvantages of the proposed solution.
2. Perform tests to understand the depth of the disadvantages and eliminate them.
3. Estimate the feasibility and further testing if required.

Thesis tasks and time schedule:

No	Task description	Deadline
1.	Perform literature review on the given topic	01.10.2019
2.	Prepare required materials and perform experiments	01.02.2020
3.	Describe experiments in detail and prepare report on results	01.05.2020

Language: ……. **Deadline for submission of thesis:** "....."..... 202….a

Student: …….. ..... "....."…….....202….a
/signature/

Supervisor: …… …….. "....."..... 202….a
/signature/

Supervisor: …… …….. "....."..... 202….a
/signature/

Head of study programme: …… ....."....."..... 202….a
/signature/

CONTENTS

PREFACE

The topic of the work was initiated by director of Naps Solar Estonia OÜ Ander Pukk and research team member of Laboratory of Thin Film Chemical Technologies Department of Materials and Environmental Technology associated professor Arvo Mere.

Solar panel lamination was done in the production facility of Naps Solar Estonia OÜ. Measurements and sample preparations were done in the Department of Materials and Environmental Technology. As the work required access to different machinery as well as knowledge, there were many people who helped with that. I would like to thank Pavel Tšukrejev and other personnel form Naps Solar Estonia OÜ who organized the sample preparations and flash test measurements. From the university side, Jako Siim Eensalu helped me with the chemicals and safety, Erki Kärber provided valuable ideas how to go forward with the work. Additionally, he helped me with the roughness measurements and finding the right people and solutions for my needs. Heinar Vagiström conducted the gritblasting for surface treatments, Andres Krumme with Illia Krasnou helped me with the peel test. Ilona Oja Açik and Malle Krunks recommended useful changes in the final work structure as they are well aware of the full picture of academic writings. Last but not least, additional contributions to the completion of this work came from the rest of the personnel of Department of Materials and Environmental Technology and my family, especially Tatjana Ots, Liisu Ots and Jane Idavain.

I wish to express special gratitude to my supervisor Arvo Mere, who has been very easy to work with. He shared honest criticism and solutions for the current work, instructed me with the process and equipment.

We acknowledge Estonian Research Council projects IUT19-4 "Thin films and nanomaterials by wet-chemical methods for next-generation photovoltaics", PRG627 "Antimony chalcogenide thin films for next-generation semi-transparent solar cells applicable in electricity producing windows" and European Regional Development Fund project TK141 "Advanced materials and high-technology devices for sustainable energetics, sensorics and nanoelectronics" for funding.

Keywords: Marine, semi-flexible, surface energy, adhesion, master thesis.

ABBREVATIONS

CTE – coefficients of thermal expansion

CZTS– copper-zinc-tin-sulfide

ETFE– ethylene tetrafluoroethylene

eV – electronvolt

EVA – ethylene-vinyl acetate

IR – infrared

I-V – current-voltage

OTR – oxygen transmission rate

PC – polycarbonate

PET – polyethylene terephthalate

PMMA – polymethyl methacrylate

PVDF – polyvilylidene fluoride

Sa – arithmetic mean height of an area

SEM – scanning electron microscopy

SFE – surface free energy

UV – ultraviolet

WVTR – water vapor transmission rate

"low-iron glass**"** – texturized and tempered silicon dioxide glass with low iron content

INTRODUCTION

Constantly growing energy consumptions has made the economy need for innovative energy production solutions and approaches. Sunlight has by far the highest technical potential of Earth's renewable energy sources that can be efficiently converted into electricity [1]. Compared to other major renewable energy resources (wind, biomass, tidal, hydro, geothermal), solar energy conversion to electricity is by far the most difficult, but most direct and potential. To produce electricity from solar radiation, photovoltaic (PV) solar cells are used – those are easily degradable by environmental factors, which is why protection of photovoltaic cells is important. Solar cells are mostly protected with glass cover. Glass has been the choice of protection due to the proved resistance against harsh environment. As new ideas, approaches and opportunities in the photovoltaic field arise, there is a need for new characteristics like flexibility and lightness. New characteristics are particularly important for marine, building integrated photovoltaic and portable device sectors. For marine sector the crucial characteristic is flexibility: most of the surfaces on marine vessels are curved and attaching rigid panels is complicated. "Semi-flexible" term is used for market dominated first-generation silicon cell solar panels, as the 16 x 16 cm silicon cells are thick and brittle, but allow moderate bending over large panel area. For this to happen, rigid glass cover has to be replaced with something flexible.

The topic is originated from Naps Solar Estonia OÜ, where semi-flexible solar panels are produced for marine applications. Current solution uses transparent and flexible polymer ethylene tetrafluoroethylene (ETFE) as the protective cover which, however, experiences certain drawbacks like high price, little mechanical protection due to its low thickness and fluctuating adhesion quality. For that reason, the main scope of this paper is to find other transparent polymers for the protective cover of semi-flexible marine solar panels. Proposed alternatives for the ETFE are commercial polymers like polycarbonate (PC) and polymethyl methacrylate (PMMA).

1. LITERATURE OVERVIEW

First part of the literature research focuses on area-specific introduction and explanation of terms in order to make understanding of the following parts easier. As the photovoltaic sector covers many aspects, presented information concentrates on information relevant for the current work. Second part of current chapter is focused on semi-flexible solar panels: market potential, research on used cover materials and requirements for front cover material.

1.1 Current status of solar power

Together with wind, biomass, tidal, hydro and geothermal, solar is one of the leading sources of renewable energy. The fact that most other renewable sources and majority of fossil energy sources originate from solar, shows the magnitude and potential of solar power. Solar energy can directly be transformed into electric energy with a photovoltaic (PV) conversion. In 2018, photovoltaics provided 2.2% of world total electricity demand. The share is still low, but there is a rapid increase in photovoltaic market: The Compound Annual Growth Rate (CAGR) of photovoltaic installations was 36.8% between 2010 and 2018, which makes it one of the most perspective renewable energy source. Leading position in PV sector belongs to Asia: according to 2017 data, China/Taiwan had a 70% share in solar panel production, USA/Canada and Europe had 3.7% and 3.1% share respectively [2].

The choice of which renewable energy source to use, often depends on aspects like location, policies, public acceptance, supportive infrastructure and so forth. Photovoltaics have achieved a position with the least restriction in implementation:

- Photovoltaics are compact, work quietly and are not visually disturbing.
- Photovoltaics are the main focus of many renewable legislations.
- Financial institutions invest preferably in photovoltaics, because production data is highly predictable [3].
- Investments are beneficial in both equatorial and polar regions.
- It can be easily installed both in rural and urban areas.

Integrating solar panels with existing infrastructure has unlocked locations with unused potential. Rooftops have found a purpose they never had: harvest energy with the help of solar panels. If sufficient solar cell efficiency and material technology is found, so could car roofs, yacht decks, roads and walls eventually be involved in electricity generation.

1.1.1 From photovoltaic conversion to solar panels

The basis of solar harvesting is the photovoltaic cell (also known as a solar cell) as shown in **Figure 1**. Initially, solar cell wafer is produced of highly pure silicon that cannot produce electric current due to the fact that all 4 electrons of silicon are bonded to the silicon lattice. After the production of silicon solar cell wafer, top of the solar cell is doped with atoms containing 5 valence electrons to create extra loose electrons in the lattice (so called n-type silicon). As a counterweight, bottom of the solar cell is doped with atoms containing 3 valence electrons to create holes in the lattice (so called p-type silicon). **Figure 2** depicts an illustrative difference between pure silicon, n-type and p-type silicon. This doping produces a p-n junction in solar cell wafer, as seen in **Figure 3** and which consist of p-type silicon, n-type silicon and a depletion zone between them. In depletion zone no excess electrons or holes exist by default, however, when light strikes the depletion zone, an electron-hole pair is produced. Automatically electron moves to the n-side and hole to the p-side due to the electric field. If many electrons and holes are produced, a potential difference is developed between n-type and p-type. As soon as we connect any load between those regions, electrons will start flowing through the load. Electrons reaching the p-type will recombine with the holes and in this way a solar cell continuously gives direct current [4].

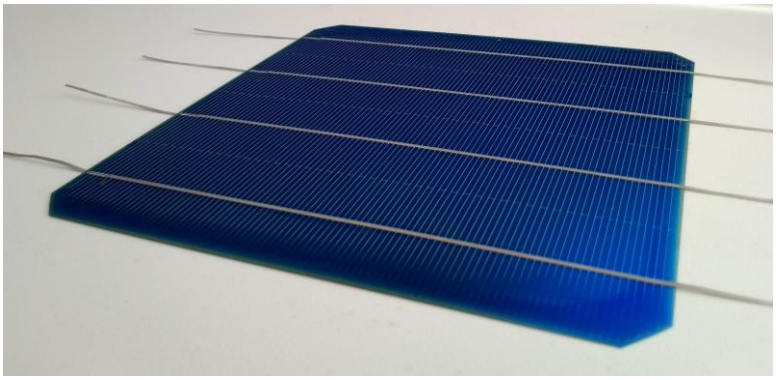

Figure 1. Basis of a photovoltaic conversion is a solar cell

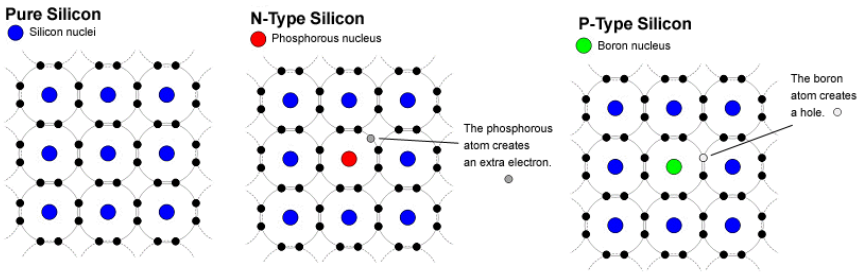

Figure 2. Difference between pure silicon lattice, n-type silicon lattice and p-type silicon lattice is the number of electrons. N-type silicon contains more electrons than pure silicon; p-type silicon contain more less electrons than pure silicon [5]

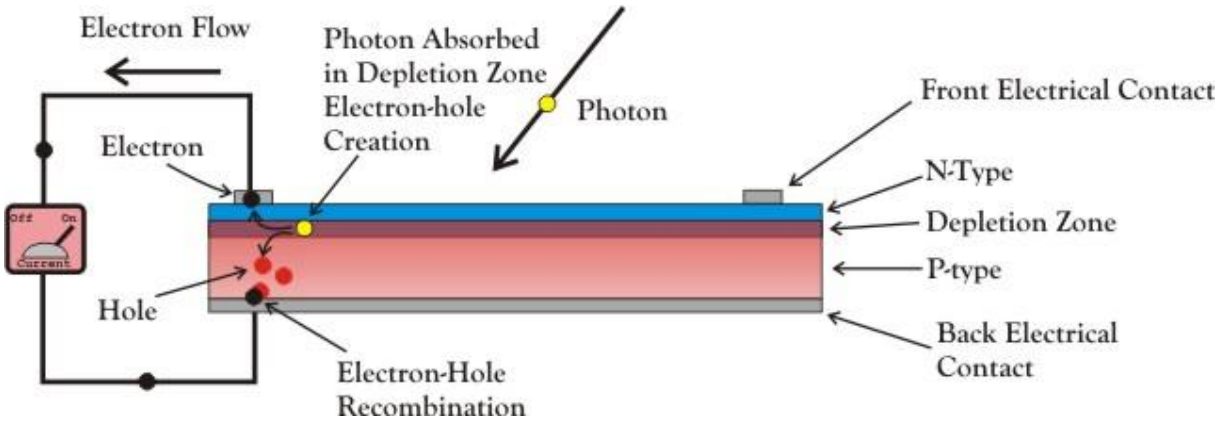

Figure 3. Cross-section view of a photovoltaic cell and its working principle [4]

Previous paragraph explained photovoltaic cell fundamentals on a silicon example. If silicon is used in a photovoltaic cell, it is known as first-generation technology. Next-generation solar cells use other materials, but are not in the focus of this work, thus no further explanation is done. First-generation silicon cells are leading the solar industry and still account for approximately 95% of the total production of the world market, with majority of that belonging to polycrystalline silicon technology [2] (silicon cells can be produced as polycrystalline or monocrystalline). Polycrystalline silicon cell consists of multiple crystals, which are each orientated in different directions. Production of polycrystalline silicon cell is cheaper, but the electrical output is lower than for monocrystalline silicon cell, which consists of only one crystal. Those cell types can be differentiated by appearance and dimensions as seen in **Figure 4**. Different crystal orientations can be seen on polycrystalline silicon cell and corners of monocrystalline silicon cells are often rounded due to technological reasons.

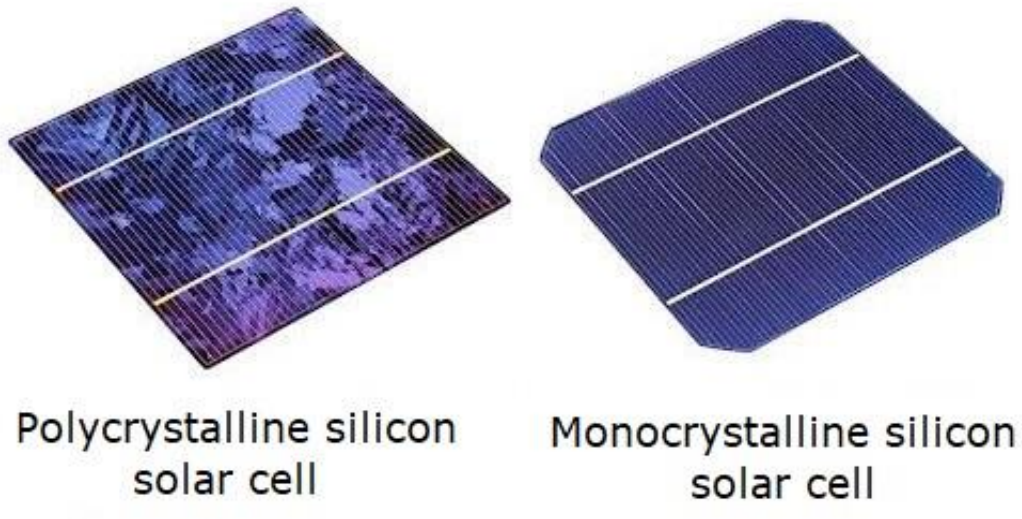

Figure 4. Visual difference between polycrystalline and monocrystalline silicon solar cell [6]

In order for solar cells to work properly for decades, they need to be well protected from environmental hazards. Multiple solar cells are connected together and protected with different materials to form a solar panel as depicted in **Figure 5**. On both sides, solar cells are covered with an encapsulant that is a hot-melt adhesive glue; mostly made out of ethylene-vinyl acetate (EVA). It is a soft rubbery polymer that glues together all layers and absorbs mechanical shocks to protect solar cells. On top, the encapsulant is covered with a frontsheet, mostly made out of texturized and tempered silicon dioxide glass with low iron content (hereinafter referred to as "low-iron glass"). On the bottom, the encapsulant is covered with a backsheet, which is made of different polymer layers. Frontsheet and backsheet provide additional protection against mechanical hazards, water and oxygen diffusion. Finally, solar panel is framed and junction box is added for wiring and electrical connections.

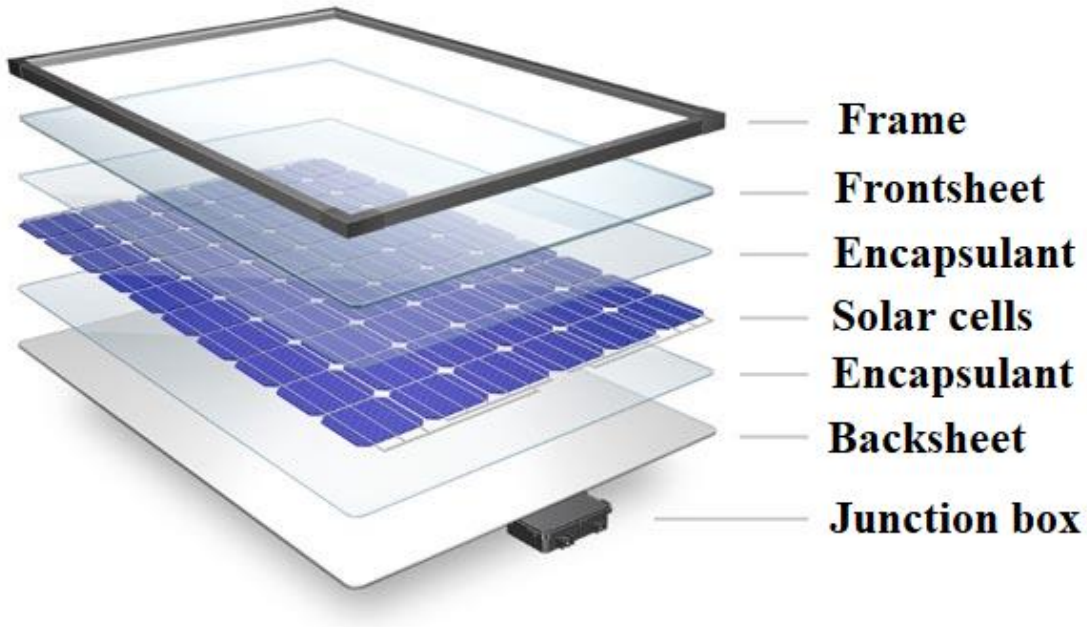

Figure 5. Structure of a solar panel [7]

1.1.2 Efficiency of a photovoltaic conversion

Once solar irradiance hits the solar cell, only about quarter of that solar energy is converted to electric energy while majority of the energy is lost in the form of heat. The highest efficiencies are achieved in laboratory environments as recorded by The National Renewable Energy Laboratory for the best monocrystalline silicon laboratory-cell with an efficiency of 26.1% [8]. Laboratory-quality solar cells however are hardly ever used in commercial solar panels due to excessively high level of silicon purification that causes the price to peak up [9]. For commercial solar panels, mass produced solar cells with

lower silicon purity are used, which possess lower conversion efficiency and lower price. Solar cells are incorporated into a solar panel, which in turn lowers the efficiency because of the following manufacturing features: empty area between cells, light blockage from busbars and wires, reflectance of the frontsheet, backsheet and the cell, optical transmission losses, resistance losses etc. Most of the previous features exist due to practical reasons and cannot be reduced much. Many solar panels that can be bought from commercial supplier have their irradiance-to-electricity conversion efficiency likely around 17% [10]. According to solar panel producers SunPower and LG, the highest efficiencies for commercial mono-crystalline solar panel in 2019 are 22.7% and 20.8%, respectively [11] [12].

1.1.3 Price of photovoltaic system

After solar cells are incorporated into a solar panel, the latter is in turn combined into a photovoltaic system that in addition to multiple solar panels consists of wiring, inverter and mounting hardware. Photovoltaic system cost per watt (€/W) is calculated from the total cost and the capacity of the system. According to photovoltaic suppliers of Estonia, the client can expect 6000 € investment for standard 6000 W residential PV system. This gives us the ratio of 1 €/W [13] [14]. However, the average price of a photovoltaic system in the United State of America is 2.7 $/W (2.5 €/W). The total cost includes price of the panels, inverter, installation, hardware (structural, electrical), inspection, permit, sales tax, net profit etc. **Figure 6** depicts the cost components of the photovoltaic system and the decrease of a total PV system cost from 2010 to 2018. Major price drop has occured for panels and installation labor [15].

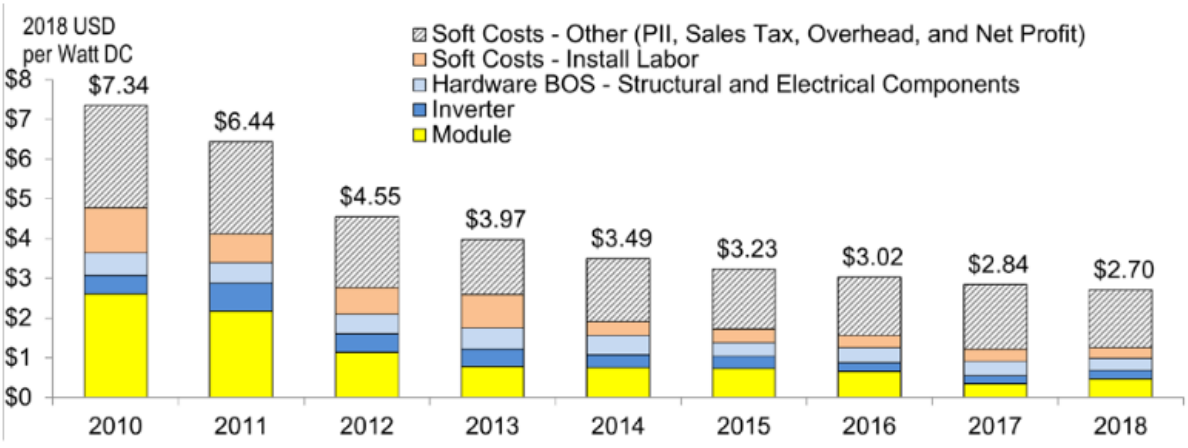

Figure 6. US Residential photovoltaic system total cost and the share of its components (inflation adjusted) [15]

From 1977 the prices of panels have decreased enormously, **Figure 7** shows the price per watt evolution in silicon solar panel production. Larger producers in Taiwan and China have managed to lower the prices of solar panels as low as 0.3 $/W by effective and cheap production and by manipulation of prices for the market domination [16]. In a commercial store, prices of solar panels vary considerably since panels are produced in various sizes and qualities. Therefore, in comparison of solar panel prices it is also appropriate to use "price per watt" formation. ENF Solar website offers a company directory with profiles of 52 148 manufacturers. In the list of ENF Solar, price for monocrystalline silicon solar panels range from about 0.18 – 0.24 €/W. However, prices are mostly shown by Asian manufacturers, European manufacturers rarely show their prices in the list of ENF Solar. Flexible solar panels, that use polymers instead of glass frontsheet, range in the same price gap [17].

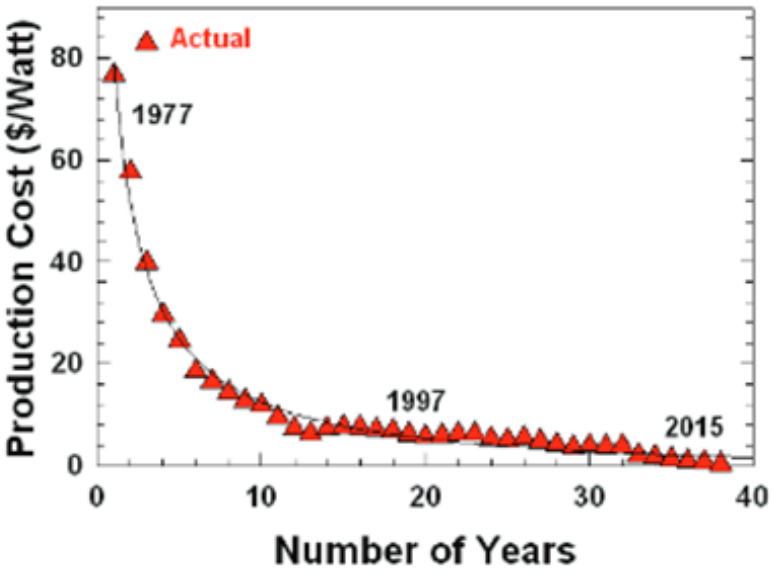

Figure 7. Historical trend of cost reduction in crystalline Si solar panel production [16]

1.2 Potential of semi-flexible solar panels

The previous part of this thesis described the overall situation, working principles and primary products in photovoltaic industry. Following sections go further into details of the solar panel structure and focus on development of certain solar panel type: semi-flexible solar panel. The potential, applications and market size are examined in the current section.

Traditional solar panels do not allow bending as it uses rigid glass cover and aluminum frame. Although rigid solar panels have worked out a reliable protection of the cells

against the outdoor environment, for certain applications rigid solar panels are not preferred. Marine sector is an example, where bendable and lightweight panels have been found to be more suitable than rigid solar panels. As seen in **Figure 8**, flat surfaces on yachts are hard to find, so semi-flexible panels are the only reasonable choice for marine sector, which according to Naps Solar Estonia OÜ is in fact one of the largest customer of semi-flexible solar panels. In the biggest e-commerce store Amazon, keyword "flexible solar panel" is typed in 14,800 times per month and for "boat solar panel" 2,400 times per month showing a moderate interest for these products. However, interest is still low, since the keyword "solar panel" is searched nearly 450 000 times per month (October 2019). Additional customers of semi-flexible solar panels come from automobile and caravan owners, off-grid portable device sector and building integrated photovoltaic sector. The director of the Estonian Renewable Energy Association, Mihkel Annus, has mentioned that in some cases traditional solar panels are not even suitable for residential buildings since they are not considered as a very attractive element anymore [18]. For those purposes the main alternatives are building integrated solar panels, where semi-flexible panels have much to contribute. In 2019, Orian Research compiled a 94-page market research report which in addition to thin film technologies cover silicon technology and propose increasing interest for flexible solar panels that can be used for boats, campers and on-the-go devices [19].

As a conclusion, semi-flexible solar panels open up applications where traditional solar panels cannot be used. Curved surfaces can easily be covered and flexibility is accompanied by a light weight and lesser thickness of the solar panel. These properties make them optically attractive and easy to carry with.

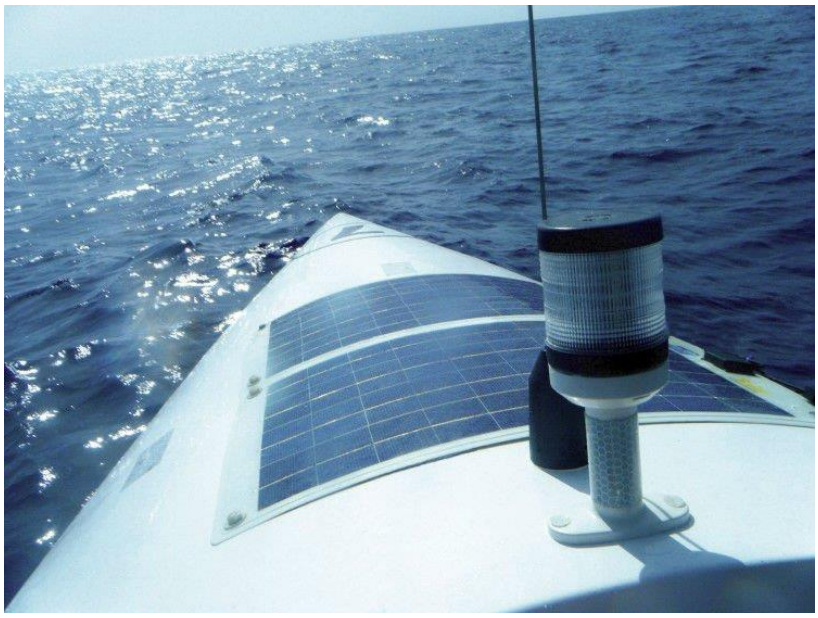

Figure 8. Semi-flexible solar panels on a yacht [20]

1.3 Frontsheet materials that are used for semi-flexible solar panels

The flexibility of a solar panel varies in relation to its construction. Highly pliable panels are known as flexible panels, less pliable as semi-flexible. Current work focuses on first-generation photovoltaic silicon cell solar panels, where flexibility is somewhat limited: the 16 x 16 cm silicon cells (**Figure 1**) are thick and brittle, but allow moderate bending over large panel area. For this reason, "semi-flexible" term is used for silicon cell solar panels. For both, flexible and semi-flexible panels, all structural components need to be made out of materials that allow flexing. The difference between semi-flexible and rigid solar panel layers (depicted in **Figure 5**) is the frontsheet material and absence of the frame. Glass frontsheet does not allow flexing and needs to be replaced with something flexible. Polymers fit that criterion well and to some extent have already been used as solar panel frontsheets. Current work is exploring the possibility of using polymethyl methacrylate (PMMA) or polycarbonate (PC) as the frontsheet of a semi-flexible solar panel. At present, ETFE is the polymer used for that purpose, which however experiences certain defects that are discussed in the end of this item.

Following part of this section concludes examples of PMMA and PC use in solar panel construction. In addition, this section describes 4 polymers that are currently most used materials for flexible solar panel frontsheets.

Polymethyl methacrylate (PMMA)

In 1982, E. Gruber released a research and development paper about encapsulation of solar cells where he compared polymethyl methacrylate, polycarbonate, celluloseester, polyamide, epoxy resin and polystyrene. He stated that PMMA is in all probability the best choice among current plastics with number of good advantages compared to glass such as low density, higher impact strength and higher transparency [21]. Chemical company Evonik Degussa is an example where PMMA is used to glaze solar panels. Patented flexible connection encapsulant is used to overcome the problem of mechanical decoupling caused by different thermal expansions. They have a successful production of PMMA lenses for concentrated photovoltaics which demonstrated the reliability and opportunity of that polymer. For thin film photovoltaics PMMA has been used as an encapsulant glue, not as a frontsheet material [22].

Polycarbonate (PC)

Tests with PC cover have been carried out by a renewables enthusiast David Losado [23], who constructed a 45-cell PC solar panel using neutral silicon as an encapsulant.

Thermal expansion and water permeability was brought out as the main reason why this concept could fail. In this case the neutral silicon could not handle the destructive effect of the ultraviolet light and failed before other factors. Martijn M. Hackmann *et al.* [24] explored the feasibility of PC solar panels and referred to a German company Solarwatt, which has experimented with double-sided PC solar panels. Public information on Solarwatt website about PC solar panels is not found. A cooperation between Sunovation GmbH and Bayer AG [25] has resulted in production of solar shades (**Figure 9**) with sizes up to 3 m x 1 m, where silicon solar cells are encapsulated between two PC sheets. Floating joints between the PC sheets ensure safe bending of the panels that can be bent to a minimum radius of 1.6 m. Another German company Galaxy Energy GmbH [26] offers flexible PC solar panel already in their product list.

Figure 9. Lamination of solar cells with polycarbonate instead of low-iron glass makes it possible to use in flexible applications [25]

Saudi Arabian petrochemicals manufacturer Sabic released a research [27] on improved reliability of PV modules with polycarbonate frontsheet. PC offers a weight advantage over low-iron glass frontsheet; compared to fluoropolymer films like ETFE, it possesses superior toughness, higher resistance to puncture and cut, low cost and higher flame retardancy - last point being a desired factor in building integrated PV solutions. Adhesion strength to encapsulant EVA achieved a value of 4 N/mm, which did not show any sign of decrease after 2000 hours of damp heat test. Sabic cooperated with PV manufacturer Solbian to elaborate PC solar panel, that was successfully used on first alternative energy based transatlantic voyager in March 2020 [28] [29].

Ethylene tetrafluoroethylene (ETFE)

DuPont, as one of the leading polymer manufacturers is producing ETFE film specially designed for flexible solar panels. According to DuPont, ETFE films have proven

performance in photovoltaic field and superior adhesion to EVA encapsulant. Higher transmittance than low-iron glass has been achieved. Thickness of 0.05 mm is already enough for protection of moisture [30]. Armageddon Energy among many others has chosen ETFE for the frontsheet material of their semi-flexible solar panels. Custom shape panel production is easier, as low-iron tempered glass cannot be cut after the tempering. Low thickness of ETFE film gives a weight advantage over traditional glass solar panel: installing 50 of those 7.7 kg panels took 40 minutes for Daytona University pilot project. Installation of traditional glass panels would have taken 2 days [31]. According to the list of flexible solar panel producers in ENF Solar, the most popular frontsheet material is in fact ETFE [17]. Naps Solar Estonia OÜ has used this polymer in their production with various results: mostly, the ETFE film is easy to laminate and provides enough protection against water and oxygen diffusion. Occasionally, the panels in the marine environment have experienced severe delamination and little mechanical protection.

Polyvinylidene fluoride (PVDF)

AI Technologies on the other hand has a polyvinylidene fluoride (PVDF) film product called SolarThru. The main advantage of PVDF over ETFE is higher light transmission and the encapsulation process is done by melting 2 PVDF panels together with solar cells in between. Less layers and materials greatly reduce the risk of delamination. That can all be done without changing the manufacturing process because laminator that is used for traditional solar panels production, can also be used for PVDF [32].

Fluorinated ethylene propylene (FEP)

FEP-based frontsheet materials are mainly produced by DuPont. Together with two previous polymers, it is a fluorine-containing polymer which has an expensive production process due to high corrosiveness. Hydrofluoric gas can be formed during thermal processing, thus, highly corrosive resistant production materials are needed. High transparency of FEP can boost the solar panel efficiency, but is prohibitively expensive [33] [34].

Polyethylene terephthalate (PET)

Polyethylene terephthalate (PET) film has already been used effectively as a backsheet of a solar panel and with minor changes it can also be used as a frontsheet of a solar panel. DuPont Teijin Films is one of the leading suppliers of polyester film and offers PET film for solar panel frontsheets under the name of Melinex [35]. After the rise of ETFE film, the use of PET is slowly decreasing as it has low moisture resistance that

results in delamination or yellowing of the encapsulant. The transparency of 80% considered too low for photovoltaic applications [36].

1.4 Requirements for semi-flexible solar panel materials

All products and their components must meet certain requirements in order to work properly, be competitive and safe. Current section brings forward different aspects, that must be considered while choosing materials for semi-flexible solar panels. Bigger emphasis is placed on frontsheet material, but as all solar panel materials have to fit together, the whole structure is kept in mind.

1.4.1 Working wavelength range of the solar cell and transparency of the frontsheet

Solar cells cannot convert all solar radiation to electric energy as solar cells have specific working wavelength range in which it is able to conduct the conversion process. For getting the most out of solar cells, the solar panel core materials that are covering the cells have to be transparent for the solar radiation in the same working wavelength range. Solar panel structure was depicted in **Figure 5** and shows that encapsulant and frontsheet are the layers in between the Sun and solar cells.

Sun emits light in the form of photons that each have their own energy measured in electronvolt (eV). Photons with enough energy are responsible for punching the valence electron away from silicon atom, making an electron-hole pair and producing electric current. Silicon cell bandgap 1.11 eV shows us that photons with energy of at least 1.11 eV is needed to knock out the electrons from a silicon atom and send it to the conduction band thus generating electricity. If the photon has more than 1.11 eV of energy, then only 1.11 eV is used effectively and the rest is converted to heat. Photons with lower energy than 1.11 eV are not capable of making an electron-hole pair and their energy is converted to heat if absorbed.

Planck's equation can be used to calculate the respective spectrum wavelength for 1.11 eV, which is 1110 nm. It is seen in **Figure 10**, that 1110 nm falls in infrared (IR) region. Anything below that (<1110 nm) silicon solar cells can use, meaning photons have enough energy to knock the electrons away from their lattice. There is however also the lowest wavelength limit for silicon solar cells. Red area in **Figure 10** indicates solar irradiation at sea level after certain amount (difference between yellow and red area) of photons are diffused, reflected or absorbed due to water vapor, air molecules

and other small particles. It is seen that the solar irradiation reaches to zero at the wavelength of around 300 nm, which is the region of ultraviolet (UV) light. Presence of anything below that (far UV, gamma rays and x-rays) at sea level is insufficient to have any affect, which is why the useful wavelength range for silicon cell is 300 – 1100 nm consisting of some amount of IR, all visible light and a portion of UV light. Solar spectrum energy share is divided into 5% UV, 43% visible and 52% IR light, which indicates that as compared to visible and IR light, the presence of UV photons at sea level is small even though the photon energy of UV light is the highest [37] [38] [39].

Based on previous information, solar cells can only work effectively if solar panel core materials are transparent for the solar radiation in the range of 300 – 1110 nm. Light transmittance of low-iron glass frontsheet and EVA encapsulant in this wavelength range is around 91% [40] [41].

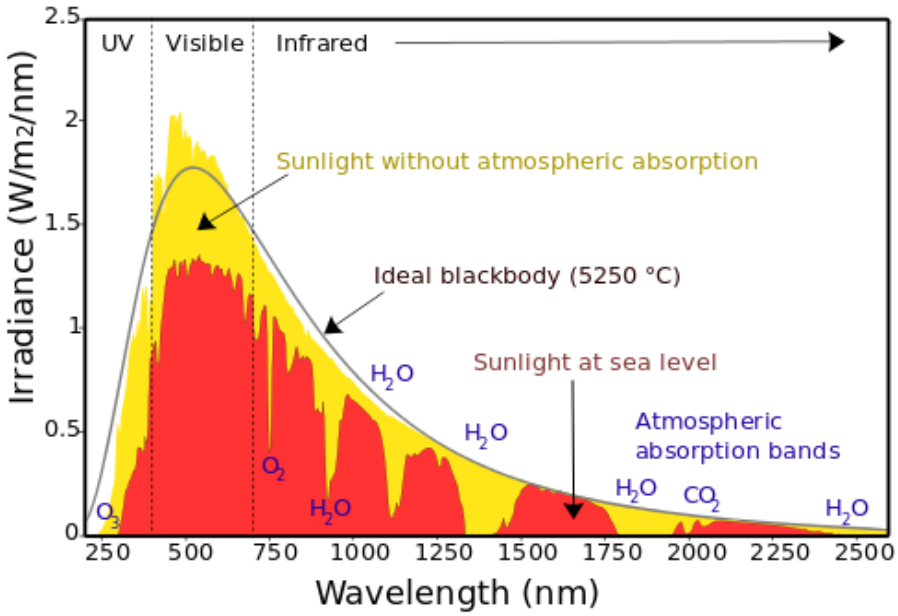

Figure 10. Solar spectral irradiance falling on Earth in the wavelength range of 250 nm – 2500 nm [37]

1.4.2 Water and oxygen resistance of frontsheet materials

Polymers have been used in photovoltaics as encapsulants and backsheets for several decades. In coming decades polymers will play even more important role when thin films and flexible panels conquer the market. Polymers used in solar systems have to be designed to protect the solar cells against an outdoor exposure for 25 years and more. Degradation of solar cells is mainly caused by photochemical reactions due to UV light, mechanical stresses and atmospheric gases (water vapor and oxygen). Oxygen and water vapor is known to be the main reason for solar cell corrosion and

photobleaching of EVA, which happens due to breakup of conjugated double bonds and is visible as yellowing or browning of EVA [42].

The permeation process is the transport of water vapor or oxygen through material. The driving force for the diffusion is the concentration differences in either side of the material membrane. The variables to quantify the permeation process are water vapor transmission rate (WVTR) and oxygen transmission rate (OTR) [42]. It is known that organic light emitting diodes require barrier with a WVTR below 10^{-6} g/ (m^2 day) and OTR below 10^{-3} g/ (m^2 day) at 25 °C and 40% relative humidity. The general perception is that solar cells require same protection rate in order to withstand outdoor environment hazards [43] [44]. The WVTR rate of the encapsulant EVA is 70 $x10^{-6}$ g/ (m^2 day), which is one of the reasons why solar cells cannot be protected with EVA solely – EVA is transmitting water vapor more than needed.

Additional aspect, that might cause problems in a solar panel, is water absorption of the frontsheet. That feature is not relevant for low-iron glass and not discussed in photovoltaic studies, but is always brought out in polymer datasheets. Polymers have tendency to absorb water over time, which can affect mechanical, electrical and dimensional properties. Wet material is known to be more permeable to gases, which certainly affects the dielectric properties of the material [45]. In a solar panel, excess absorption of polymer frontsheet could decrease the adhesion strength in frontsheet-encapsulant interface.

1.4.3 Thermal expansion of solar panel materials

The feature, currently examined in here, is the thermal expansion of solar panel layer materials. When solar panel layers are laminated together with the temperature of ~150 °C and then cooled to room temperature, the layers of different materials expand and contract differently. This movement creates stresses that cause curving of the panel, delamination or breakage of fragile cells.

Material tendency to change shape in a fluctuating temperature environment is called thermal expansion, that is expressed with coefficient of linear thermal expansion (CLTE or CTE). For initial comparison, the coefficient gives a clear overview of the differences [46]. **Table 1** presents the coefficients of linear thermal expansion for traditional solar panel layer materials. Silicon cell has a very low CTE which means its dimensions do not change significantly during the lamination process. The highest value of CTE is for EVA encapsulant, which does not induce significant stresses for the panel due to its low stiffness. Backsheet has also a relatively high value of CTE and wants to contract after lamination. Low thickness of the backsheet does not allow that, because low-iron glass

frontsheet on the other side of the solar panel has higher stiffness and thickness. Low-iron glass is around 73% by weight made out of SiO2, so its CTE value is similar to pure silicon and it does not significantly change its dimensions during lamination [47]. As can be concluded, low-iron glass is the reason why traditional solar panels are planar. Using other materials instead of low-iron glass frontsheet with different CTE values can deteriorate the harmonization, unbalance the stresses and result in a curved panel. Thermoplastic polymers for instance have CTE values around 60 x10-6 /K to 230 x10-6 /K [45].

Table 1. Linear thermal expansions coefficients of various solar panel layer materials

	Coefficient of linear thermal expansion, x10^{-6} /K
Low-iron glass	8.9 [48]
Silicon solar cell	2.6 [49]
Ethylene-vinyl acetate (EVA)	180 [50]
Backsheet	100 [45]

Finite element thermal stress analysis made by Lee Yixian and Andrew A. O. Tay [51] shows measurable stress even for traditional solar panels that use low-iron glass frontsheet. When the temperature of the laminator is achieved, the panel is in stress-free state. After encapsulation and during cooling, the materials of solar panel contract differently. Is has been stated, that temperature decrease from 145 °C to 30 °C results in bowing of the traditional solar panel of about 1.16 mm outwards at the center of the panel (dimensions of the solar panel were 1580 mm x 790 mm). That displacement reflects to the radius of 67 m. The study concluded that internal stresses existing in glass panel could cause problems after years of outdoor exposure. Because of low expansion coefficient and high stiffness of low-iron glass, displacement is small and stresses are not large enough to cause cracks in the solar cells. The fact that CTE values for polymers frontsheets are ~10 times higher can be responsible for numerous malfunctions [51].

A paper written by Martijn M. Hackmann [24] describes a feasibility study of PC solar panels, where test panels with different configurations were modeled in order to understand the influence of thermal expansion. Following changes in solar panel configuration were made:

(1) Increasing the thickness of EVA encapsulant from 0.4 mm to 1.2 mm.
(2) Reducing the thickness of PC frontsheet from 5 mm to 3 mm.
(3) Lamination without the backsheet (product name TPT).

(4) Using different backsheet (product name Halar).

(5) Encapsulating without solar cells.

(6) Using one large silicon cell with dimensions of 1180 mm x 540 mm.

Finite element analysis of those configurations allowed to see the extent of the solar panel curvature (**Figure 11**). Z displacement shows the displacement perpendicular to the solar panel surface with the center of the panel fixed to 0 mm. It turned out using thicker PC and EVA reduces the bending as thicker PC provides higher stiffness and thicker EVA provides higher degree of stress relaxation. Large silicon cell increased the curving, whereas encapsulation without cells ended up with bending to the opposite side, meaning that using smaller size solar cells could result with minimal stress thus less bending. Different backsheet variants did not influence the curvature. Thicker PC sheet (5 mm) and thicker EVA layer (1,2 mm) achieved bending radius of 5±1 m and 7,5±1 m respectively [24].

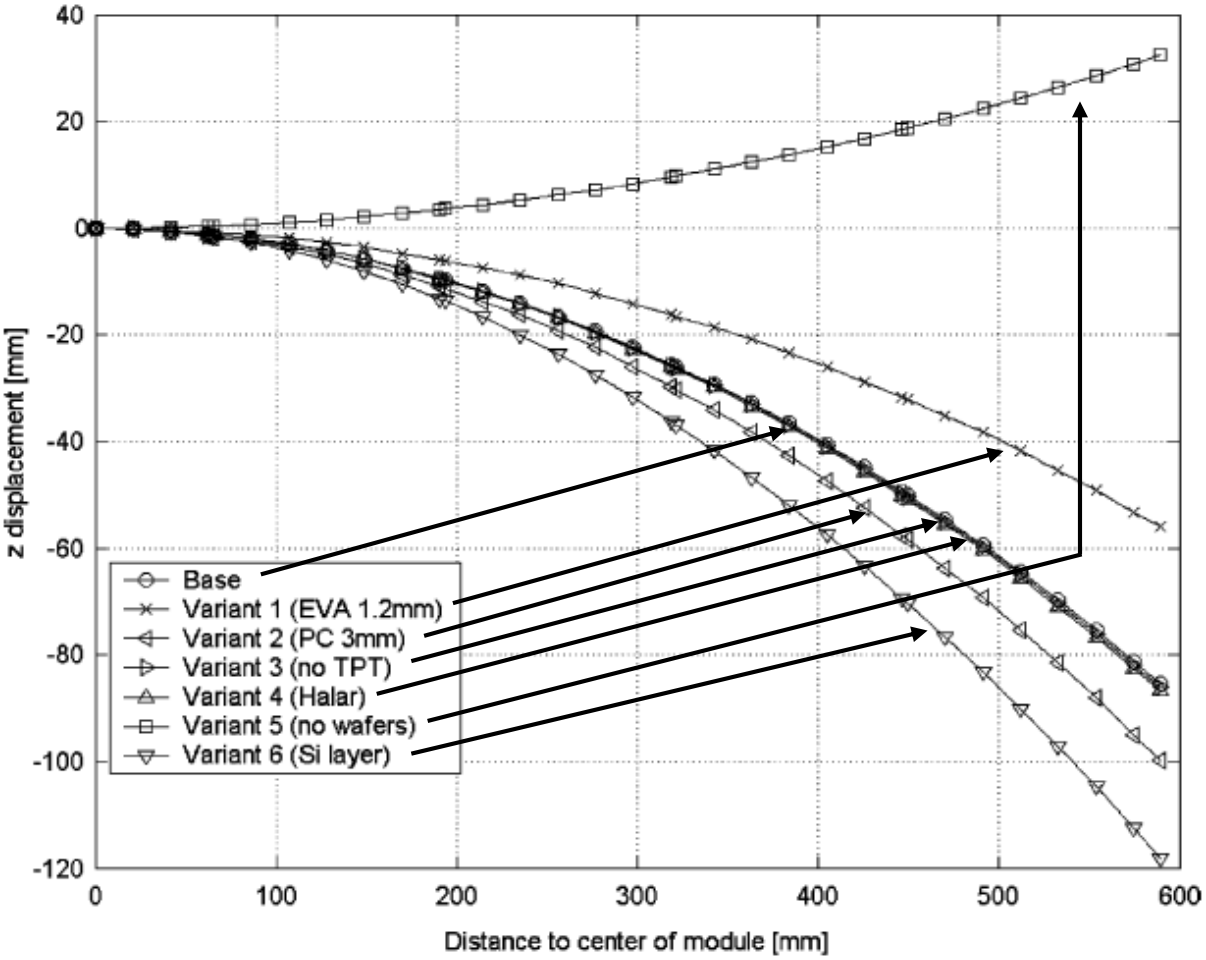

Figure 11. Different solar panel configurations produce different extent of solar panel curvature after lamination and a temperature step from 100˚C to 20˚C that. Curving is seen as z displacement perpendicular to the surface of the laminate [24]

1.4.4 Temperature resistance of the frontsheet

During the manufacturing process of solar panels, different layers are fused together in a laminator which uses vacuum to remove the air between layers and temperature of around 150 °C to melt the EVA and fuse together all the layers. Traditional solar panels can easily withstand that temperature, but while changing the materials, one has to consider the temperature of lamination process [52]. Polymers have maximum continuous working temperature commonly around 100 °C – 150 °C [45]. Before melting, some polymers with amorphous structure (like PMMA and PC) experience glass transition where material transforms from solid into rubbery. If the melting temperature or glass transition temperature of the frontsheet material is lower than the temperature of lamination process, the material appearance will be affected.

1.4.5 Adhesion between solar panel layers

For about 30 years, the material-of-choice for solar panel encapsulation has been hot-melt adhesive ethylene-vinyl acetate (EVA) and nearly 80% of photovoltaic panels are assembled with that. EVA is a thermoplastic copolymer that on its own does not fulfill adhesion requirements. By crosslinking copolymer chains, a suitable encapsulant is formed. For a standard solar panel, the encapsulant is in contact with the low-iron glass frontsheet, silicon cells and backsheet. The main function of the encapsulant is to attain superior adhesion with all the elements of solar panel. It is stated that the lifetime of a solar panel is determined not by limits of photovoltaic process but by moisture transmission into the panel. To limit early degradation, a good adhesion is necessary. Replacement of the low-iron glass might create a situation where EVA does not produce sufficient bond with the new material due to the fact that EVA has been chemically modified to be used with glass. If low-iron glass is replaced with polymers, extra care has to be taken as polymers are difficult to adhere and often result in poor adhesion [52] [53] [54].

Mechanisms of adhesion

Adhesion is the molecular force interaction between different phases or materials, which result in sticking to one another. Molecular forces categorize into intramolecular (primary) and intermolecular (secondary). Primary forces consist of strong ionic, covalent and metallic bonds inside a molecule, which are usually not active in the case of adhesion. Secondary forces consist of weaker hydrogen and van der Waals bonds between molecules, that apply most in the case of adhesion [55]. Adhesion is a complex phenomenon - the main responsible mechanisms are still being argued about and researchers classify them differently. Overall question is: what assures a good adhesion?

Some of the mechanisms from literature are mechanical interlocking, diffusion, adsorption, electrostatic, thermodynamic, acid-base, chemical bonding, physical interaction etc. As seen, some are more in depth, some general – they do not exclude each other. Some interactions like Van der Waals forces can be classified under physical, electrostatic or adsorption mechanism. It is often difficult to describe adhesion with a single mechanism and often a combination of different methods are believed to be responsible [56] [54] [57].

Expected adhesion strength for encapsulant-frontsheet interface

The most common adhesion strength measurement methods in PV sector are 90° peel test, 180° peel test and shear test. National Renewable Energy Laboratory has tested adhesion strength with 90° peel test between EVA and low-iron glass with values between 9 – 14 N/mm and 180° peel test with a value around 12 N/mm. Effects of glass type, texture and surface cleaning has not been obvious [41] [58]. Another source finds similar results with the value of 14 N/mm adhesion strength between glass and EVA [59]. Specialized Technology Resources considers EVA-glass adhesion strength ≥5.3 N/mm sufficient [60]. Another conference paper that researched photovoltaic panel lamination durability tested EVA glass adhesion with 90° test, where the results showed average strength of 7.5 – 12.5 N/mm [53].

Surface treatment effect to adhesion strength

Adhesion of untreated polymers is often too low for practical applications. To increase the adhesion ability, following surface treatments and promoters are used: chemical, plasma, corona discharge, flame, UV, mechanical treatment. Chemical treatment increases surface polarity, which causes an increase in molecular forces between the materials. Toluene, xylene and acids have been used for the most basic pretreatments. Soaking polymers in hydrochloric acid solution has resulted in increased adhesion strength by highly polar carboxyl groups. Plasma treatment allows us to change the properties of the polymer surface without changing the bulk. Reaction between plasma and polymer surface creates oxygen-containing polar groups such as (C=O), (CO), (COO), (OH) and (OOH). Those chemically reactive groups increase the surface energy and wettability, which in turn may improve the adhesion to other materials [54]. Trivial methods like surface roughening are also an option for increasing adhesion, however in solar panel frontsheet applications, there would be a side effect in transparency drop.

Kazimierz Drabczyk [61] conducted adhesion strength test of PMMA-EVA with different surface treatments like PMMA grinded with P80 sandpaper, PMMA grinded with P120 sandpaper, satin type PMMA and clear PMMA with laser net of cuts. Abraded surface

may increase the adhesion due to one or more of the following factors: mechanical interlocking, increased contact surface area, formation of highly reactive surfaces and formation of clean surfaces. **Figure 12** shows the test results of Kazimierz Drabczyk, which concluded that sandpaper treated surfaces (E2, E3) were able to increase the adhesion quality as compared with clear PMMA (E1), while satin surface (E4) resulted in poorer adhesion. It has to be noted that chemically designed polymers have a wide variety of different properties that cannot be easily compared. Same researcher did another test with polyvinyl butyral (PVB) encapsulant and satin PMMA, in which an increase of adhesion strength was recorded instead [61].

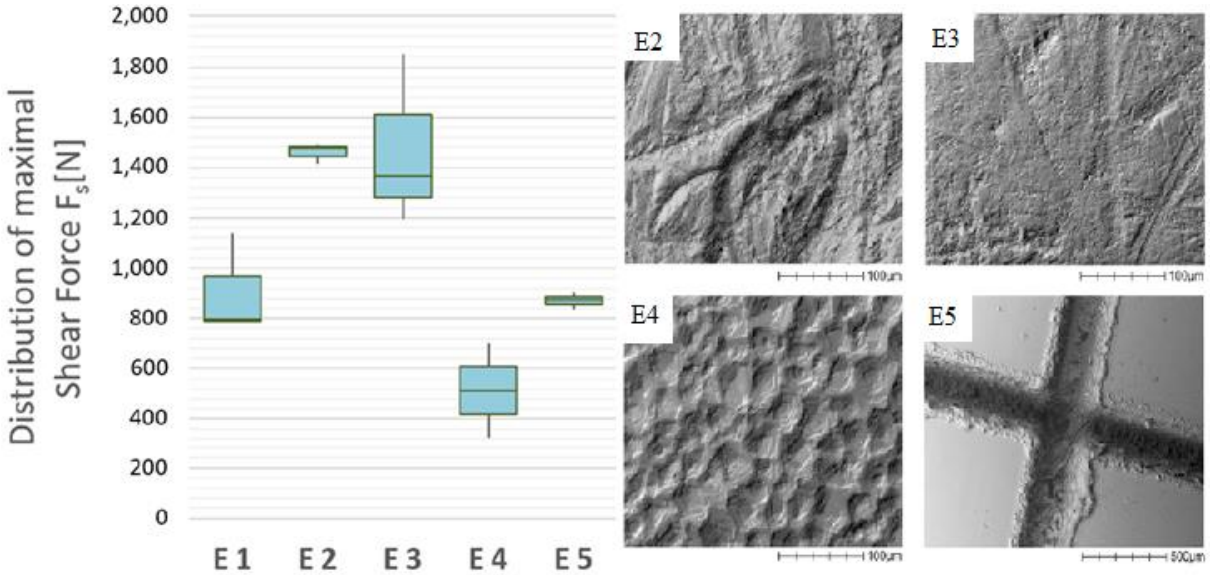

Figure 12. Left side of the figure indicates shear test values between ethylene-vinyl acetate (EVA) and frontsheet material with various treatments like (E1) clear PMMA, (E2) P80, (E3) P120, (E4) satin, (E5) laser cuts. Right side of the figure shows scanning electron microscopy (SEM) images of the same frontsheet treatment surfaces [61]

1.4.6 Price of the frontsheet

Solar panel industry is constantly expanding and getting more competitive. In order to increase margins, manufacturers are eagerly searching for cost-cutting options and materials with performance advantage. Attention has been turned to structural materials like backsheets, frontsheets and encapsulants. Backsheet color for instance can significantly influence the total performance of the solar panel [33].

Lux Research compiled a report for alternative frontsheet materials and their influence to the performance of the solar panel (**Figure 13**). Many alternatives were actually able to increase the solar panel efficiency, however with an average of 20 – 40% higher price. Difference to competitive price was calculated from current material cost and break even cost. The latter was calculated by evaluating the impact of solar panel

efficiency. For some materials, the efficiency increase did not pay off the higher material price. Long-term environmental performance was not evaluated [33].

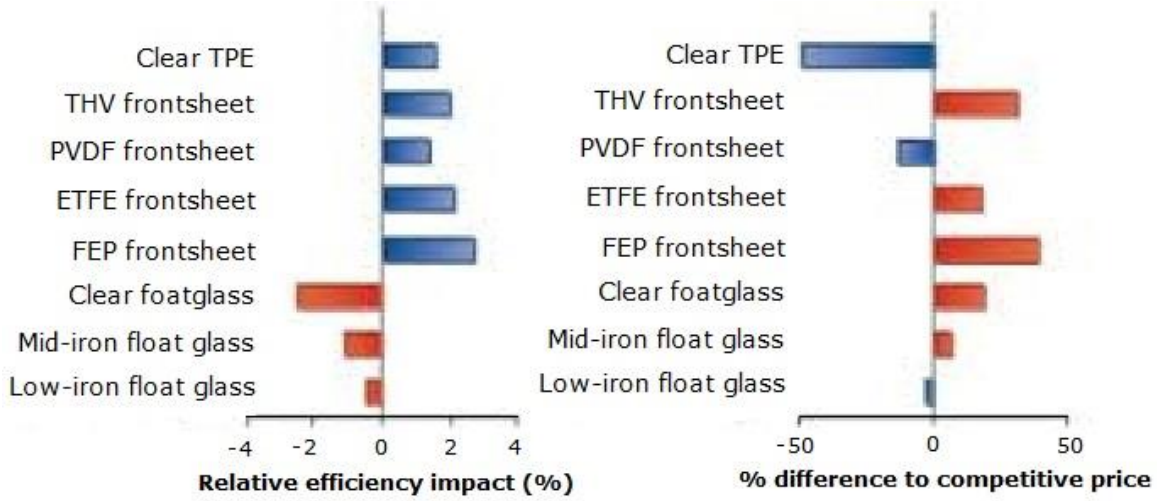

Figure 13. Efficiency and price effect if low-iron glass frontsheet is replaced with alternative materials.(PVDF - polyvilylidene fluoride; ETFE - ethylene tetrafluoroethylene; FEP - fluorinated ethylene propylene [33]

1.5 Summary of literature review and aim of the work

Semi-flexible solar panel is a niche product in the photovoltaic industry with primary market in marine, caravan and portable device sector. Development of solar panel flexibility requires material alternatives for the rigid glass frontsheet cover. The alternative frontsheet material must have high transparency in order to avoid the decrease of the solar cell efficiency in its working wavelength of 300 – 1110 nm. For comparison, light transmittance of glass frontsheet in this range is 91 %. Solar panel encounters high temperature fluctuations (from 150 $^{\circ}$C to 20 $^{\circ}$C) in the manufacturing process. This is problematic for polymers, which naturally have higher thermal expansion as compared to glass frontsheet and silicon solar cells. Such difference induces stress between the layers that result in curving of the panel, delamination of layers or breakage of fragile cells. Superior adhesion of solar panel layers is necessary in order to protect solar cells against outdoor environment. Adhesion strength of 5,3 N/mm and above for frontsheet-encapsulant interface has been found acceptable. Historically, polymers experience low adhesion to other materials, which can be significantly improved with surface treatments. Consensus on responsible adhesion mechanisms has not been achieved by scientists. As a result of previously mentioned requirements, the alternative flexible frontsheet material must be carefully selected. Ethylene tetrafluoroethylene (ETFE) is currently the main substitute for the glass frontsheet in semi-flexible solar panels. ETFE has relatively high price, provides little mechanical protection due to its thin film and has occasionally experienced severe

delamination. Several alternatives such as polymethyl methacrylate (PMMA) and polycarbonate (PC) have been proposed, which both have a long history in outdoor use. There are examples of them used in solar panels, however manufacturers keep the details and technology classified.

Based on literature review and Naps Solar Estonia OÜ need, the aim of the master thesis is to evaluate the feasibility of using commercial PMMA and PC as a frontsheet cover of semi-flexible solar panel for marine applications.

The specific objectives to achieve the aim are:

1. To compare possible frontsheet materials' properties: PC and PMMA against low-iron glass and ETFE.
2. To test PC and PMMA frontsheet in solar panel. Main focus on structure integrity and the effect of thermal expansion of stacked layers.
3. To test surface treatments of PC and PMMA in order to improve their adhesion to encapsulant. Simultaneously, investigation of treated surfaces will be carried out to determine the prerequisites of an adequate adhesion with encapsulant to simplify labor-intensive adhesion strength test, which is currently determined with peel test.

2. EXPERIMENTAL DESCRIPTION (APPARATUS, METHODS AND SAMPLE PREPARATION)

Second chapter is divided into two parts from which the first explains the process of preparation works and second focuses on different methods of characterization.

2.1 Preparation of solar panels and sample surfaces

2.1.1 Preparation and manufacturing of solar panels

Certain tests in this work required preparation of miniature solar panels (370 x 540 mm) containing 6 monocrystalline silicon cells. Monocrystalline silicon cell with dimensions 156 x 156 mm were of Chinese origin. Ethylene-vinyl acetate (EVA) encapsulant was used as a hot-melt adhesive to fuse solar panel layers together. Frontsheet material PC was produced by Koscon Industrial S.A. and PMMA by Polycasa N.V. Configuration of solar panel layers varied according to the purpose of the test. The preparation of solar panels was made in manufacturing unit of Naps Solar Estonia OÜ, who provided monocrystalline cells, laminator, testing equipment and industrial knowledge.

Manufacturing of a solar panel requires vacuum and high temperature to (1) remove air between layers and to (2) melt and crosslink EVA encapsulant. This is provided with a vacuum lamination, as depicted in **Figure 14.** All test panels were put into the laminator with frontsheet side of the solar panels facing towards the heating elements. Lamination time and temperature depends on various factors: materials used, power of the laminator, desired degree of EVA crosslinking. 70% of crosslinking is considered adequate in most cases. [53]. Traditional solar panel with low-iron glass frontsheet takes 140 $^{\circ}$C and 20 minutes in Naps Solar Estonia OÜ. The same cycle was chosen for this work.

Figure 14. High temperature vacuum laminator for the manufacturing of solar panels [62]

2.1.2 Preparation of sample surfaces

Several tests of the current work focused on adhesion between frontsheet (in this case PMMA or PC) and encapsulant EVA. Adhesion is highly influenced by the surface of materials, thus altering of frontsheet surfaces was conducted to examine the effect of different surface treatment methods to adhesion ability. Information about different surface altering treatments that apply to PMMA and PC was gathered from literature and are as follows: sandpaper, gritblasting, flame, UV and chemical treatment [63] [64] [65] [61] [57].

More detailed explanation of chosen surface treatments and preparation of samples are presented in bullet points below and concluded in **Table 2.** Abbreviations presented in table will be used in further parts of this work in mentioning the different surface treatments.

- Sand paper and gritblasting were chosen as they are supposed to increase the adhesion since EVA flows into the voids and interlocks itself to the base material. Increase in surface contact area can also increase the total adhesion. Sand paper grits P60, P120 and P240 were used with an average particle diameter 269, 125 and 58.5 micrometers respectively. Particle diameters for aluminum oxide (Al_2O_3) gritblasting were 25 and 100 micrometers. Treatment time of 5 minutes provided a uniform surface.
- Flame treatment is based on creating plasma in the oxygen-rich hot flame, which is similar to plasma treatment and corona treatment, where plasma is generated in a non-thermal way. Activated molecules bind to the surface and produce (RCOOH) and (ROH) functional groups which increases the molecular interactions between frontsheet and EVA [66]. Flame treatment is a quick and cheap method – top layer of the test pieces is slightly melt with blue propane flame.
- UV treatment is often used to clean surfaces from impurities. UV treatment initiates the chain scission of polymer groups, after which an increase in (ROH), (RCOR'), (RCOOH) and (ROOH) hydrophilic functional groups have been noticed when examined with x-ray photoelectron spectroscopy. SEM pictures of UV treated polymer surfaces have shown increase in roughness and porosity [65]. For UV treatment, Novascan PDS UV ozone cleaner was used to irradiate the samples for 15 minutes with UVC radiation with wavelength of 253.7 nm, which provides 28 – 32 mW/cm^2. Distance from the lamp was 5 cm.
- Chemical treatment by sulfuric acid and chromic mixture is supposed to increase hydrophilicity by introducing (RSO_3H), (ROH) and (RCOOH) groups to the polymer chain. Increased hydrophilicity is measured with surface free energy as for PC it could be increased from 43 mN/m to 87 mN/m. 4 different sulfuric acid

based receipts were tested. For PMMA, 12M sulfuric acid was used for 5 and 30 minutes. As PC is more resistant to sulfuric acid, 18M concentrated sulfuric acid and chromic mixture was used both for 5 minutes. Chromic mixture is often used for cleaning laboratory glassware and was prepared by adding concentrated sulfuric acid H_2SO_4 to sodium dichromate salt $Na_2Cr_2O_7$ in a 22:1 ratio by weight [64] [57] [67].

Table 2. Concluding table presents the applied surface treatments for PC and PMMA for further tests. Abbreviation of treatments will be used in further part of this work in mentioning the different surface treatments. Treatment time refers to duration of specific treatment on the sample.

		Applied to:		
Abbreviation	**Treatment**	**PMMA**	**PC**	**Treatment time**
Control	No treatment	x	x	-
P60	Sandpaper P60	x	x	5 min
P120	sandpaper P120	x	x	5 min
P240	sandpaper P240	x	x	5 min
100 µm	Al_2O_3 gritblast, 100um	x	x	5 min
25 µm	Al_2O_3 gritblast, 25um	x	x	5 min
UV	UVC lamp	x	x	15 min
Flame	Oxygen-rich flame	x	x	2 sec
12M 5’	12M H_2SO_4	x		5 min
12M 30’	12M H_2SO_4	x		30 min
18M 5’	18M H_2SO_4 (conc.)		x	5 min
Cr 5’	Chromic mixture		x	5 min

2.1.3 Preparation of peel test samples

Preparation for peel test required lamination of the frontsheet materials with encapsulant EVA and backsheet as seen on peel test sample (**Figure 15**), dimensions of the peel test specimen will be explained in **Item 2.2.4.** Peel test samples were all laminated at the same time in Naps Solar Estonia OÜ. Due to technical reasons, the time between frontsheet material surface treatment and lamination of the samples was not the same for all treatments. Time was therefore recorded for every treatment and can be seen in **Table 3**. Recording time is important because some surface treatments like UV and Cr 5’ can lose their effect over time.

Figure 15. An example of 180º peel test specimen consists of rigid adherent (frontsheet) and flexible adherent (encapsulant + backsheet)

Table 3. Time between frontsheet surface treatment and lamination of the peel test sample. **Table 2** in previous section further explained the abbreviations of surface treatments

Abbreviation of surface treatment	Time between surface treatment and lamination, hours
P60	5
P120	5
P240	5
100 µm	5
25 µm	5
UV	1.5
Flame	3.3
12M 5’	29
12M 30’	29
18M 5’	29
Cr 5’	29

2.2 Characterization of solar panels and frontsheet surfaces

2.2.1 Optical measurements

Jasco V-670 UV-VIS-NIR spectrophotometer was used to measure transmittance of solar panel frontsheets (PMMA, PC, low-iron glass and ETFE) and haze of PMMA and PC surface treatments.

Transmittance measurement provides information about material's ability to pass through light. Spectrophotometer light source produces electromagnetic spectrum in UV, visible and IR light range, and measures the light transmittance of material for each wavelength. Useful wavelength area for silicon cell was discussed in **Item 1.4.1**, which was from 300 – 1100 nm. The lower wavelength limit 340 nm was chosen for the measurements, because the transmittance of PC and PMMA dramatically drops already before 300 nm, thus, if 300 nm had been used instead of 340 nm, no useful information would have been received.

As an addition to transmittance measurement, spectrophotometer was used for haze measurements, as this is a useful method in determining surface structure change after surface treatment. As an addition to roughness, light is scattered because of porosity, crystal structure, impurities, mechanical and chemical degradation. Haze is a percentage of light that is scattered more than 2.5° through the sample and can be calculated by the ratio of total light transmittance T_t and sample diffusion T_d with the following equation [45] [68]:

$$Haze\ factor = \frac{T_d}{T_t} \times 100\% \tag{2.1}$$

2.2.2 Surface free energy measurements

Surface free energy (SFE) is a measure of excess energy on the surface of a material and is used to describe adhesion and wetting between materials. Increase in surface free energy denotes increase in wetting, but does not necessarily lead to improved adhesion as there are many types of forces occurring while two materials are in contact. Wetting is still important when it comes to initiating adhesion and is therefore proposed as a useful parameter in coating and gluing processes [56] [69]. In the current work, the adhesion interface between frontsheet and encapsulant was under examination (the layers a solar panel were depicted in **Figure 5** in the literature review). In the following part contact angle (wettability) of a surface and surface free energy is explained in detail.

Contact angle analysis

Contact angle analysis gives an understanding about the surface wettability, after which SFE can be calculated based on wettability values. Contact angle analysis is using optical sessile drop method (**Figure 16**) to measure the angle between the tangent of the liquid drop and surface of the examined solid (so called wettability). For this purpose, Krüss DSA25 was used to find contact angle of distilled water and diiodomethane on the

surface of frontsheet materials (low-iron glass; ETFE; PC and PMMA treated surfaces). For most appropriate comparison, contact angle of molten EVA should have been used, but as this required unavailable equipment, alternative test liquids were used. Two test liquids (water and diiodomethane) were needed for calculation that is explained in the next paragraph.

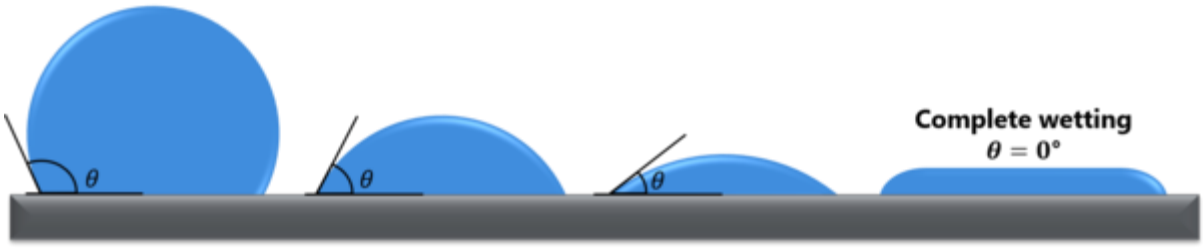

Figure 16. Optical sessile drop method is using a liquid drop on solid surface to measure the contact angle (θ) between the solid surface and tangent of the drop.

Surface free energy calculation

Contact angle values can be used to calculate the surface free energy of the solid. Over the years, different calculation methods have been proposed, Owens and Wendt method has been chosen for this work as this method is suitable for moderately polar surfaces [69] [70].

In Owens and Wendt two component model, SFE is divided to polar and dispersive contributors. Dispersive part theoretically accounts for van der Waals and other non-site specific interactions that a surface is capable of having with applied liquid. Polar part theoretically accounts for hydrogen bonding, dipole-induced dipole, dipole-dipole and other site-specific interactions. **Figure 17** illustrates the fact that dispersive part of a solid can only interact with the dispersive part of a liquid; same applies for polar part. No interaction between dispersive and polar part is possible. Blue part on the illustration symbolizes polar and yellow disperse interaction. As seen, total surface free energy σ of 50 mN/m is divided to polar ($\boldsymbol{\sigma^p}$= 10 mN/m) and dispersive ($\boldsymbol{\sigma^d}$= 40 mN/m) part. As dispersive part cannot interact with polar part, it is important for us to know the ratios in frontsheet surface energy [71] [72].

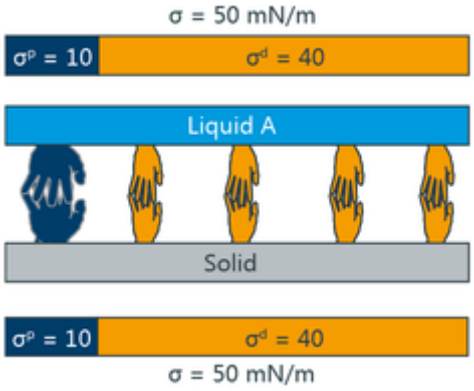

Figure 17. According to Owens and Wendt model, surface free energy σ is divided to dispersive $\boldsymbol{\sigma^d}$ and polar $\boldsymbol{\sigma^p}$ part. Illustrative sketch shows possible interactions between dispersive and polar part [72]

Owens and Wendt method requires at least two test liquids with known polar and dispersive part. Therefore, if we obtain polar and dispersive value of at least two test liquids and the contact angle data of those liquids on the investigated solid, then we will receive all the information needed to use the Owens and Wendt equation in the form of y = mx + c: [69]

$$\frac{\sigma_l(cos\theta + 1)}{2(\sqrt{\sigma_l^D})} = \left(\sqrt{\sigma_S^P}\right)\frac{\sqrt{\sigma_l^P}}{\sqrt{\sigma_l^D}} + \sqrt{\sigma_S^D} \tag{2.2}$$

Where θ – contact angle of the liquid on the solid, °

σ_l – surface tension of the liquid, mN/M

σ_l^D – dispersive component of the surface tension of the liquid, mN/M

σ_l^P – polar component of the surface tension of the liquid, mN/M

σ_S^D – dispersive component of the surface tension of the solid, mN/M

σ_S^P – polar component of the surface tension of the solid, mN/M

Figure 18 depicts a graph that can be plotted in the form of previous equation to calculate the dispersive and polar component of surface free energy of the solid. Gradient of a best line is used for finding the polar part and interception for the dispersive part of the SFE of the solid [71] [70] [69].

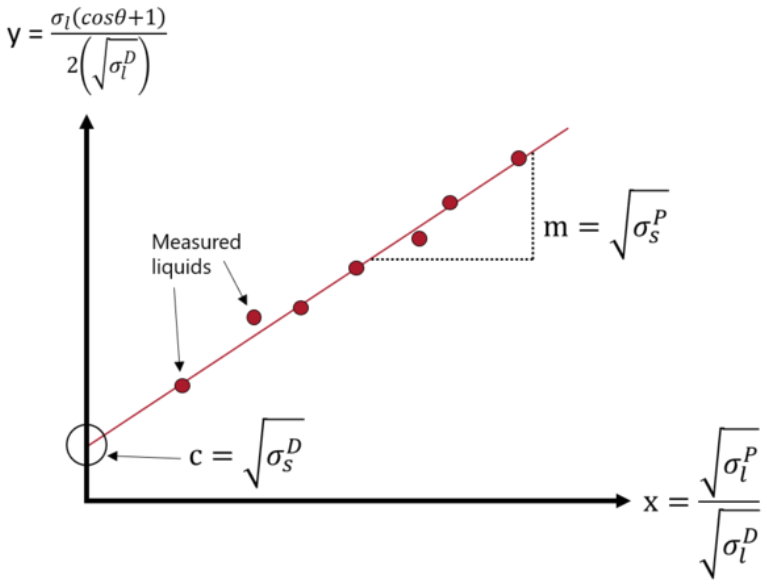

Figure 18. Owens and Wendt plot in the form of equation (2.2); surface energy components can be found from the gradient of a best line and intercept [69]

Data of test liquids is presented in **Table 4,** that shows the dispersive part $(\gamma\frac{d}{L})$ and polar part $(\gamma\frac{p}{L})$ of the test liquids water and diiodomethane, which were taken from Krüss DSA-4 database. Water possesses high share of polar part, which means it can easily wet polar materials. Diiodomethane, on the other hand, is a dispersive liquid with polar share of 0 mN/m.

Table 4. SFE dispersive and polar components (mN/m) for selected contact angle test liquids

	$\gamma\frac{d}{L}$, mN/m	$\gamma\frac{p}{L}$, mN/m
Water	21.0	51.0
Diiodomethane	50.8	0

2.2.3 Surface roughness measurements

Roughness measurements were done with Bruker GT profilometer that uses the principles of interferometry to gather information about the vertical heights on the surface. As a result, a 4,830 µm x 3,623 µm area was scanned, from which a 3D image and data were obtained. Arithmetic mean height of an area (*Sa*) is the extension of arithmetic mean height of a line (*Ra*) that expresses the difference in height of each point compared to the arithmetical mean of the surface. This value is most often used to express the roughness of an area [73].

2.2.4 Adhesion strength measurements

Adhesion strength between encapsulant and frontsheet is measured with 180º peel test, which follows EVS-EN 8510-2:2010 standard. **Figure 19** shows the set of the peel test: frontsheet as a rigid adherent and encapsulant (EVA) + backsheet as the flexible adherent. Backsheet is added to the flexible adherent to prevent the rupture as the encapsulant is thin and easily torn. Together, the adherents are thick enough to withstand the applied tensile forces. Minimum length of 225 mm is used for the rigid adherent and 375 mm for flexible adherent. In this way the adhesion length for two substrates can be at least 150 mm. Width of the specimens is 25 ± 0,25 mm according to the standard. In this test 10 ± 0,25 mm is used due to the fact that a reference peel test has already been done between low-iron glass and EVA by NAPS with the width of 10 mm. Values of peel strength are converted to N/mm for universal comparison. Recommendable speed for the tensile test machine is 100 ± 10 mm/min [74]. Peel test was conducted with mechanical testing machine Instron 5866.

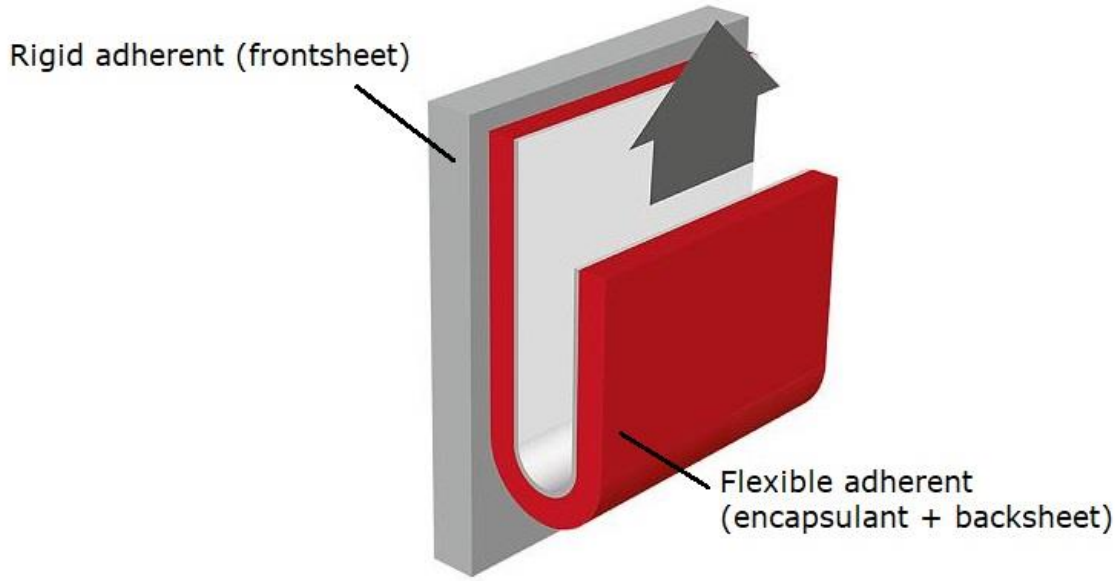

Figure 19. 180º peel test for the determination of adhesion strength between the interface of solar panel cover (frontsheet) and glue (encapsulant) [75]

2.2.5 Measurement of the curving radius

Item 1.4.3 discussed panel curving due to thermal expansion differences and ways to reduce the curving radius. As this research is using polymer frontsheets with high thermal expansion and low stiffness, curving is an inevitable byproduct of the lamination process.

Different solar panel configurations were laminated and the radius of the curved panel was found by measuring panel length and curved panel center point deviation from flat panel center point. **Figure 20** gives an illustrative idea how the radius of an arc (red line) is related to right triangle (blue triangle).

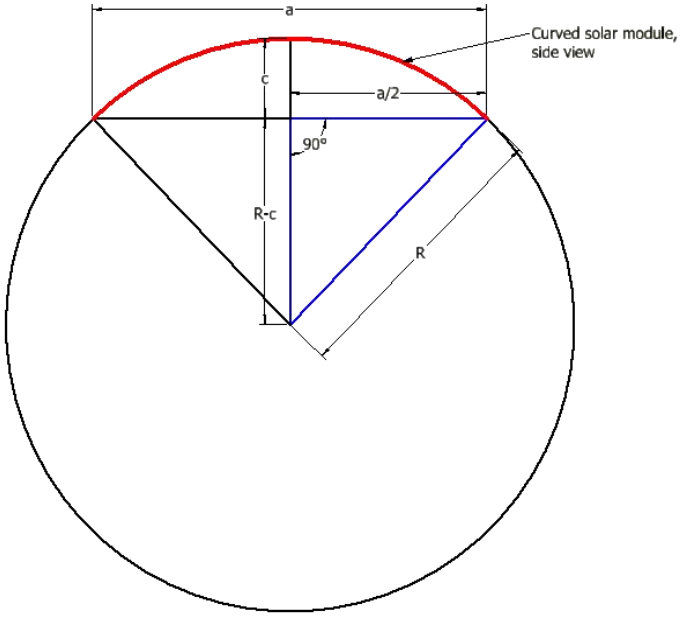

Figure 20. Relation between radius of an arc, chord and right triangle.

When panel curve is considered as part of the circle arc, Pythagorean theorem can be used in finding the radius of the curvature with a following equation:

$$R = \frac{c}{2} + \frac{a^2}{8c} \tag{2.3}$$

where R – radius of the arc, m

a – panel length projection on the ground, m

c – curved panel center point deviation from flat panel center point, m

2.2.6 Electrical measurements

Solar panel electrical measurement is summarized with current-voltage (I-V) scan (also known as the flash test). Flash test uses a lamp that produces 1000 W/m^2 to simulate the spectrum of the Sun as exactly as possible. Exposure of the Sun in real conditions differs greatly due to many aspects so the 1000 W/m^2 exposure is agreed by institutions to make comparing possible and uniform. An example test report for a low-iron glass solar panel is shown in **Figure 21**, which produces a current-voltage (I-V) curve. The

graph gives useful information about open circuit voltage, short circuit current, fill factor, maximum power point and efficiency. The relationship between current and voltage makes it possible to calculate and compare the differences in solar cell efficiency due to optical dissimilarities of various frontsheets.

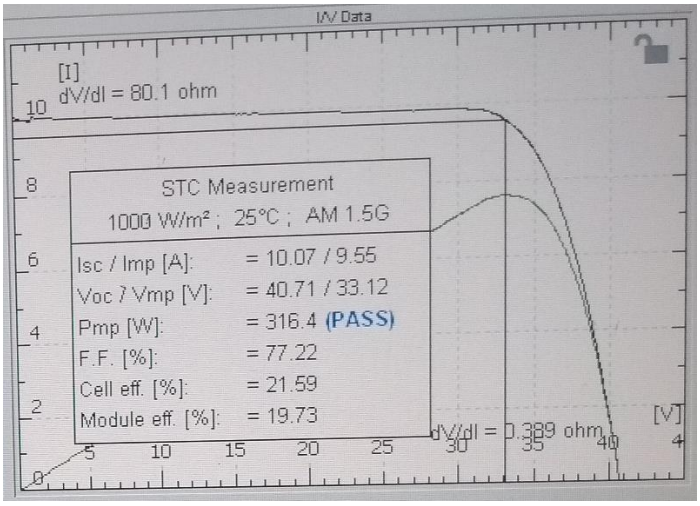

Figure 21. An example I-V curve and output parameters for a standard low-iron solar panel

3. RESULTS AND DISCUSSION

3.1 Comparison of possible frontsheet polymers

For current work, PMMA and PC was chosen as the alternative materials for semi-flexible solar panel cover (frontsheet). PMMA and PC are not in wide commercial use for solar panel covers, but possess various good properties that has made it sensible to investigate them. Low-iron glass and ETFE was chosen as the reference materials as low-iron glass is used in traditional rigid solar panels and ETFE is currently used in semi-flexible solar panels, but it experiences minor problems that were discussed before (**Section 1.3**). In this section, the feasibility of PMMA and PC is examined according to available material data. Some performance influencing properties that are relevant for outdoor use of photovoltaics and lamination are brought out in **Table 5** and discussed in the following items.

Table 5. 4 solar panel cover (frontsheet) materials and some of their properties, that are relevant for this work [76] [77] [78] [79] [80] [40]

	Polycarbonate (PC)	**Poly(methyl methacrylate) (PMMA)**	**Tempered low-iron glass**	**Ethylene tetrafluoroethylene (ETFE)**
Light transmittance, %	88	93	90	93
Water absorption, %	0.4	0.2	~0	0.02
Water vapor transmission rate, x10^{-6} g/(m^2 day)	115	55.2	~0	7.8
Coefficient of linear thermal expansion, x10^{-6} /K	65	75	8.5	90
Melting point, °C	230	160	1,500	270
Glass transition, °C	145	110	726	n/a
Hardness, Vickers	220	290	669	93
Density, kg/m^3	1,200	1,190	2,500	1,700
Approximate price, €/m^2 / thickness, mm	15 / 3*	12 / 3*	7 / 3,2*	24 / 0,1*

n/a – value not found, * - Material price per thickness

3.1.1 Optical properties

According to the knowledge of **Item 1.4.1**, solar panel core materials that are covering the solar cells, have to be transparent for the solar radiation in the range of 300-1,110 nm. Transparency (or transmittance of light) is measured in percentages and shows how much sunlight is passing through the material; the rest is either reflected or absorbed [45].

Transmittance of PC, PMMA, low-iron glass and ETFE were found from the datasheets of those materials (presented in **Table 5**), which indicate the transmittance plateau in visible light and infrared (IR) region. In addition, datasheets included transmission-wavelength graphs, that provided information about the transmittance drop in ultraviolet (UV) region (UV cut-off). A summarizing sketch of all graphs was compiled in **Figure 22**, showing the transmittance plateau and UV cut-off wavelength of PMMA, PC, low-iron glass and ETFE. The transmittance of low-iron glass, that is used in traditional rigid solar panels, is around 90% with a UV cut-off wavelength at 350 nm. Transmittance of ETFE is around 93% in the visible light range and no sudden drop is recorded in the UV range: transmittance gradually decreases to 80% when reaching to wavelength of 350 nm. Realistically, there is no need for high transmittance in far-UV range, as the portion of low wavelength light on Earth's surface is insignificant. For PC, the transmittance is 88%, which is the lowest of all displayed materials; transmittance drops near 400 nm. PMMA transmittance according to the data sheet is 93%, which exceeds the value of low-iron glass. UV cut-off is in the same region as for PC at around 400 nm. For regular PMMA and PC, the transmittance in UV range is reduced on purpose, since there is always a problem of polymer degradation by UV light if UV-reducing agents are not added. For special purposes, the transmittance in UV region could be increased – Crylux offers a custom type PMMA-UVT which is traditionally used in solarium machinery and has a UV cut-off wavelength at 325 nm [76]. In addition to frontsheet transparency, it is appropriate to investigate the transparency of encapsulant, as this layer is also situated between the Sun and the solar cells. The most used encapsulation glue EVA has a transmittance plateau of around 90 – 92% with a UV cut-off wavelength at 340 – 400 nm. In the product datasheets, the UV cut-off is often shown with the term UV cut-off / UV filtering", which is a reminder that excessive UV light leads to degradation of EVA [81] [41].

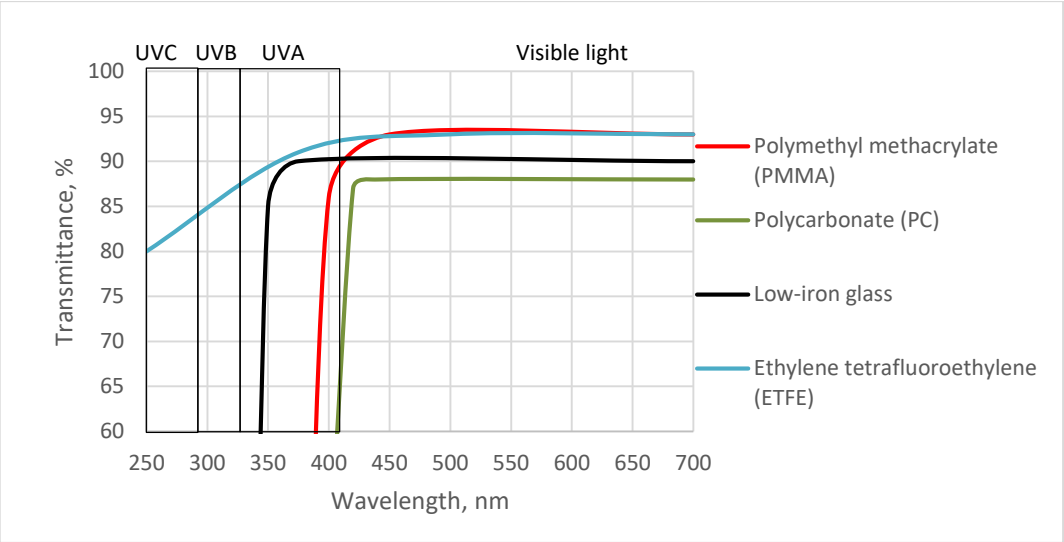

Figure 22. Transmittance behavior of frontsheet materials in the wavelength range of 250 – 700 nm. Sketch compiled according to literature data [40] [78] [77] [76]

Datasheets of frontsheet materials do not provide information about the thickness of measured materials, which highly influences the transmittance. For this reason, separate transmittance measurement was conducted for a comparison purposes. Thickness of materials were chosen according to industrial practice: 3.2 mm is the usual thickness for glass cover, whereas 0.012 – 0.125 mm thickness is used for ETFE cover. Thickness of 3 mm was chosen for PMMA and PC cover. **Figure 23** shows transmittance curve of PC (3 mm), PMMA (3 mm), low-iron glass (3.2 mm) and ETFE (0.04 and 0.1 mm; measured by the author. Transmittance plateau of PC is 88% from 425 – 1100 nm; UV cut-off wavelength is at 425 nm. PMMA has a steady transmittance plateau with 92% and UV cut-off wavelength at 390 nm. Low-iron glass has an average transmittance of 90% with a UV cut-off wavelength at 350 nm. Transmittance of 0.004 mm ETFE is around 93% from 340 – 1100 nm; 0.1 mm ETFE transmittance at high wavelengths is around 92% and starts a gradual drop below 800 nm until reaching transparency of 85% at 340 nm. Overall transmittance values match with the ones from the literature, however, following remarks can be seen: (1) transmittance of PC and low-iron glass do not have a steady plateau, (2) ETFE thickness influences the transmittance considerably.

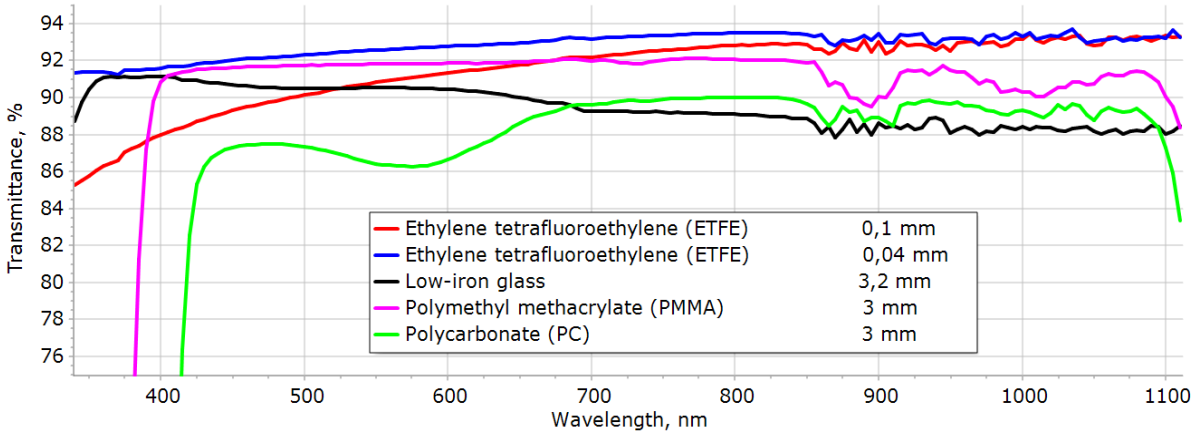

Figure 23. Measured transmittance behavior of frontsheet materials (with thickness) in the wavelength range of 3400 – 1100 nm

The results of transmittance review and measurements show the lowest transmittance for PC (88%), but relatively high transmittance for PMMA (92%). Low transmittance of PC does affect the electrical output of a solar cell, but for some applications 87% transmittance could still be acceptable. UV cut-off wavelength of both, PMMA and PC was higher than for low-iron glass and ETFE; ideally the lowest UV cut-off wavelength value is preferable, meaning more UV light is transmitted through the material. On the other hand, high transmittance of UV light can induce the degradation of solar cells and encapsulant. This aspect could cause problems for ETFE, that has high transmittance in UV region. Both graphs (**Figure 22** and **Figure 23**) show an interesting trade-off in the comparison of PMMA and low-iron glass: PMMA has a higher transmittance plateau value, but transmit less UV light (high UV cut-off wavelength); the situation is opposite for low-iron glass. Higher transmittance plateau should be superior, as UV region (<400 nm) only contributes ~5% to ground level spectrum energy [37]. In overall, commercial PMMA and PC are found suitable for solar panel cover, the feasibility could be increased by using thinner material and custom composition that increase the transmittance plateau and lowers the UV cut-off wavelength.

3.1.2 Water resistance

1.4.2 explained the problems associated with water vapor transmittance and absorption. A comparison of frontsheet materials follows in this item along with data presented in **Table 5**. Replacing the low-iron glass that has a vapor transmittance rate (WVTR) of ~0 $x10^{-6}$ g/(m^2 day) with a polymer, turns solar panel much more susceptive to water vapor, as glass is known to be hermetic, but polymers not. Among the presented polymers, ETFE experiences the lowest WVTR value; the same applies for absorption percentage. In a comparison between PC and PMMA, the latter proves to be

a safer choice in terms of water resistance, as the WVTR of 55.2 $x10^{-6}$ g/(m^2 day) is two times lower than for PC. The difference in water absorption is small, but still has to be considered (0.2% for PMMA and 0.4% for PC).

Studies from Polymer Competence Center Leoben GmbH [77] point out a fact, that moderate permeability of solar panel materials is still necessary, as otherwise yellowing of encapsulant EVA is increased. In a traditional solar panel, the permeation process occurs through the polymer backsheet, as the low-iron glass frontsheet does not allow diffusion. For solar panels with low-iron glass backsheet and frontsheet, the necessary diffusion is disturbed and increased degradation of encapsulant EVA has been noticed.

To summarize, precise conclusions on water resistance cannot be drawn based only on the material's properties. Environmental test would in this case can give further understanding on the effects of water vapor transmittance and absorption.

3.1.3 Thermal properties

Thermal properties that are relevant for solar panel materials, are glass transition temperature, melting temperature and coefficient of linear thermal expansion (CTE). **Item 1.4.3** covered basics and problems; discussion about the material data is followed in this item.

Current work uses encapsulant glue EVA with recommended lamination temperature of 140 °C. As seen from **Table 5**, low-iron glass can easily withstand that temperature. This is not the case with some of the polymers: at temperature 110 °C PMMA turns from glass to rubbery and affects the appearance of the material. The material can still retain its basic form, as the melting starts at 160 °C. PC has a higher melting temperature of 230 °C and glass transition temperature of 145 °C, which should not cause problems during lamination. Stable C-F bonds in ETFE are probably the reason for having much higher melting temperature of 270 °C [82].

All flexible frontsheet materials (ETFE, PC and PMMA) have high coefficient of linear thermal expansion (CTE) as seen from **Table 5**, which results in notable dimension change during the lamination process. This, in turn, induces high stress between layers and can result in curving of the panel. To estimate the magnitude of curving, practical tests were done and will be presented in the following part of this work. Curving depends on CTE and stiffness of the material, cooling rate of different panel sides, stress relaxation points etc. [24]. In industrial practice, ETFE is used in semi-flexible solar panel and no problems with high CTE have been noticed. The difference from the panels in this work is the very low thickness of ETFE (0.012 – 0.125 mm).

To summarize, thermal properties of PMMA and PC by far raise the most concern in regards of the feasibility of these materials. Low temperature resistance could be resolved with low temperature encapsulants that require ~110 °C for the curing process. Thermal expansion part however does not provide straightforward solutions, thus practical testing is needed for precise conclusion.

3.1.4 Physical and mechanical properties

Solar panels must withstand harsh environments where abrasive particles, rocks, branches etc. over time reduce the transparency or break the front cover. Here, three properties are discussed: hardness, brittleness and weight.

Hardness (presented in **Table 5**) gives useful information about the scratch resistance of the material. Tempered low-iron glass has hardness of 669 on Vickers scale while PMMA, PC and ETFE have 290, 220 and 93, respectively. Low hardness of polymers can definitely affect the long-term transparency of a solar panel, which in turn reduces the power production. In principle, polymer hardness could be slightly increased with scratch resistant coating but not as much to compete with glass.

Additional comparison could be made on material's brittleness: when stress is applied to a brittle material, it breaks with little or no plastic deformation. In this aspect PMMA and PC have a fundamental difference, as on room temperature PMMA behave like a brittle material, whereas PC as a ductile (**Figure 24**). This means shattering of PC frontsheet is practically impossible.

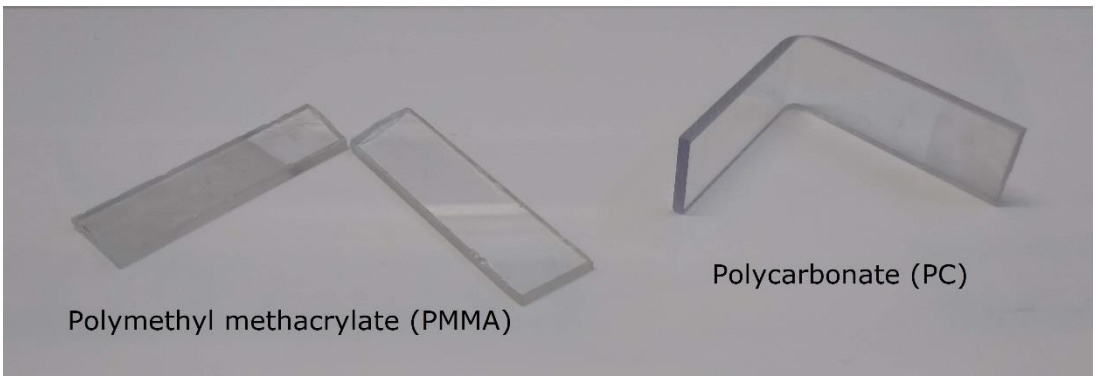

Figure 24. One of the difference between PMMA and PC is their brittleness

It is clearly seen from **Table 5**, that low-iron glass frontsheet is a denser material than polymers and increases the total weight of the solar panel. By using the thickness and dimensions of a traditional solar panel cover (3.2mm and 986 x 1623 mm), the weight of a low-iron glass frontsheet is 12.8 kg, whereas weight of PMMA / PC frontsheet would be 6.1 kg. Weight contribution of ETFE is insignificant, because according literature

findings, thickness of 3.2 mm has never been used; typical thickness of ETFE film is 0.012 – 0.125 mm [78].

To summarize, PMMA and PC can offer useful advantages to solar panel development, but inevitably there are trade-offs in the form of low hardness. PC experiences excellent durability against mechanical forces, whereas PMMA act in the same manner as low-iron glass. Weight is a definite advantage over traditional low-iron glass even in non-flexible solar panels concepts.

3.1.5 Price

As discussed in **Item 1.4.6**, manufacturer's attention has been turned to non-active materials of solar panels (backsheet, frontsheet, encapsulant) – reducing their price and improving their performance is crucial in competitive market. Getting realistic and accurate price of frontsheet materials is not easy, as it highly depends on market situation and order volumes. Information was gathered with the help of Naps Solar Estonia OÜ and Proplastik OÜ. Approximate frontsheet material prices per square meter are presented in **Table 5**, note that materials have different thicknesses. Thickness of materials was chosen according to industrial practice: 3.2 mm is the usual thickness for glass cover, whereas 0.012 – 0.125 mm thickness is used for ETFE cover. 3 mm was chosen for PC and PMMA according to low-iron glass thickness, but ideally thinner material could be used. In this case the price would also decrease: 1.5 mm thick PC and PMMA would cost approximately 8.3 €/m^2 and 7 €/m^2 respectively.

Considering the gathered information, commercial polymers offer a considerable price advantage over ETFE (price: 24 €/m^2) and are relatively price competitive compared to low-iron glass.

3.2 Testing of chosen materials in a solar panel

According to the comparison of frontsheet material properties, both PMMA and PC were found suitable for semi-flexible solar panel purposes. This section starts with the practical testing, where prototype solar panels were prepared using PMMA or PC frontsheet instead of low-iron glass to understand the overall nature and problems of a polymer covered panel. Evaluation of prepared solar panels was done similarly with manufacturing practice: by visual examination and measurement of electrical parameters.

Lamination

Figure 25 depicts the configuration of the prototype solar panel layers. Test panels contained 6 silicon cells, using PC or PMMA frontsheet cover, standard backsheet (product name: "Tedlar") and hot-melt encapsulant EVA. Thickness of 3 mm was chosen for PC and PMMA as in traditional rigid solar panel the low-iron glass is 3,2 mm thick. Further details of the lamination was described in **Item 2.1.1.**

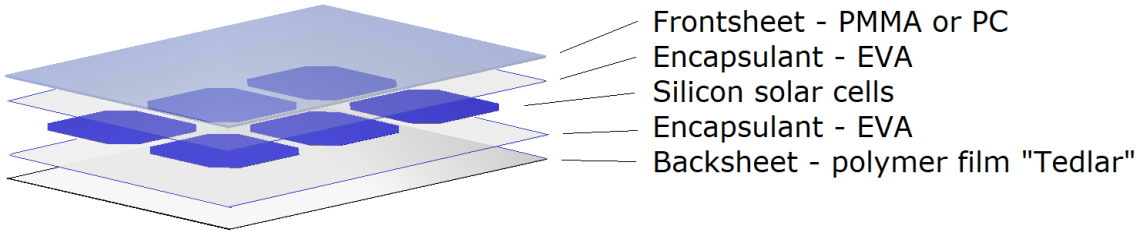

Figure 25. Configuration of the test solar panel layers (EVA – ethylene-vinyl acetate, PC – polycarbonate, PMMA – polymethyl methacrylate)

Visual examination

Coming out from the laminator it was clear that PMMA started softening as laminator pattern was imprinted onto the surface of PMMA frontsheet. The softening of PMMA was expected to happen, since the glass transition point of PMMA is lower than lamination process. As seen in **Figure 26**, both panels were curved and interestingly in opposite directions. When the panels start cooling from 140 °C, the material with the highest coefficient of thermal expansion (CTE) shrinks the most, leading to bowing. The panel consists of following layers and thermal expansion coefficients:

- Front: PC/PMMA and EVA encapsulant (high CTE)
- Between: Cells (very low CTE), tabs and cell metallization (low CTE)
- Back: EVA encapsulant and backsheet (high CTE)

The front and back layer shrink more than cell layer. As the front layer is thicker than back layer, this side is expected to be dominant. For this reason, all panels should bow like PC. In an e-mail conversation with researcher Kees Broek from Netherlands Organization for Applied Scientific Research, he explained his work with PMMA lamination where 1 out of 3 panels bowed like the PMMA panel in this work. As for this 1 panel, thicker and stiffer encapsulant was used; the preliminary conclusion was that the stress difference in the front and back layer was significantly reduced. Therefore, the panel had more chance to bow in the unexpected direction. For this work, the same encapsulant was used, so stresses are most likely in a balance state and direction can be determined by a small stimulus.

A week after the lamination PMMA frontsheet started delaminating from EVA. Three weeks later the whole frontsheet was delaminated. PC, on the other hand, had no issues.

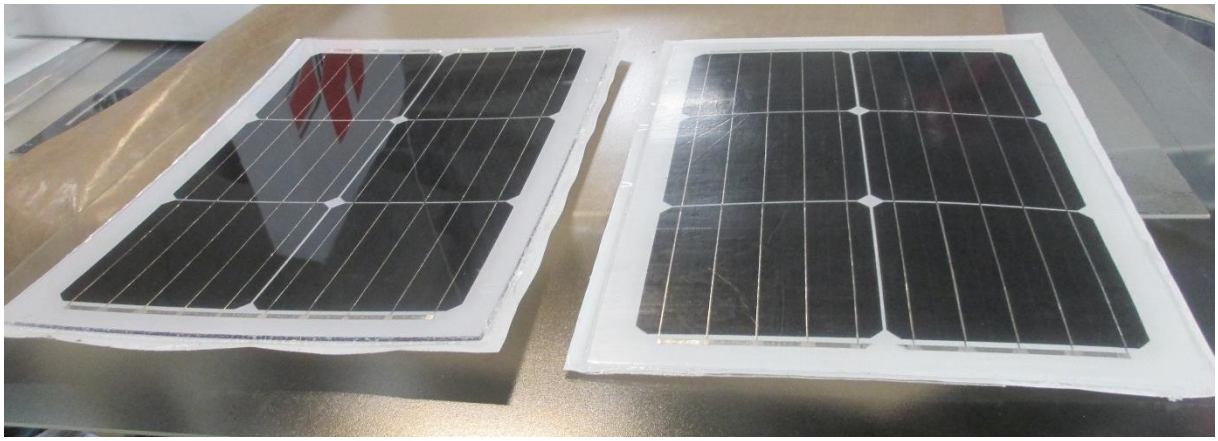

Figure 26. Test solar panel after the lamination. Left with polycarbonate (PC) and right with polymethyl methacrylate (PMMA) frontsheet. Curving of two panels were in opposite directions

Electrical measurements

Item 2.2.6 explained the basics of flash test and the information received by that. Both of the prototype solar panels were measured and results compared with the values of a low-iron glass solar panel. The reference low-iron solar panel was a full size 60-cell panel, which means that not all parameters were comparable. Cell efficiency, however, is well comparable as it shows the efficiency of 1 solar cell. **Table 6** shows the results of cell efficiency of the prototype panels and the low-iron glass panel. PC solar panel experiences the lowest cell efficiency, which can be related to a low transmittance. Reference low-iron glass panel showed 1.64% higher cell efficiency value as PMMA panel, despite the fact that light transmittance of PMMA is ~2% higher than low-iron glass. This could show that UV-light region still plays a vital role, because low-iron glass experiences lower UV cut-off wavelength than PMMA. Difference could also come from texturized surface and anti-reflective coating that the low-iron glass has.

Table 6. Cell efficiencies of polymethyl methacrylate (PMMA), polycarbonate (PC) and low-iron glass solar panel

	PMMA solar panel	**PC solar panel**	**Low-iron glass solar panel**
Cell efficiency	19.95%	18.74%	21.59%

3.3 Testing of different configurations of a solar panel layers

Item 1.4.3 discussed panel curving due to thermal expansion differences and ways to reduce the curving radius. As this research is using polymer frontsheets with high thermal expansion and low stiffness, curving is an inevitable byproduct of the lamination process. First part of this section describes the lamination of test panels and second part presents the curving radius measurements and conclusions.

Lamination

For the testing of curving, 3 different configurations (named as A, B and C) for solar panel layers were made as depicted in **Figure 27** to evaluate if curving radius could be reduced. In this test, only PC was chosen for a frontsheet material, as PMMA exhibited poor adhesion to encapsulation glue. Configuration A uses a similar layering that is used for a traditional solar panel with 3 mm front cover (frontsheet). Configuration B uses symmetrical layering with 3 mm cover on both sides of the panel. Configuration C uses symmetrical layering and 5 mm polymer cover on both sides of the panel. Symmetrical layering should balance the stresses evenly, thus reduce the bending of the panel. Increasing the thickness of front and back cover should reduce the bending even more. Panels were laminated in Naps Solar Estonia OÜ by using the vacuum laminator regime 140 °C and 20 minutes. Frontsheet side of the panels was facing towards the heating elements.

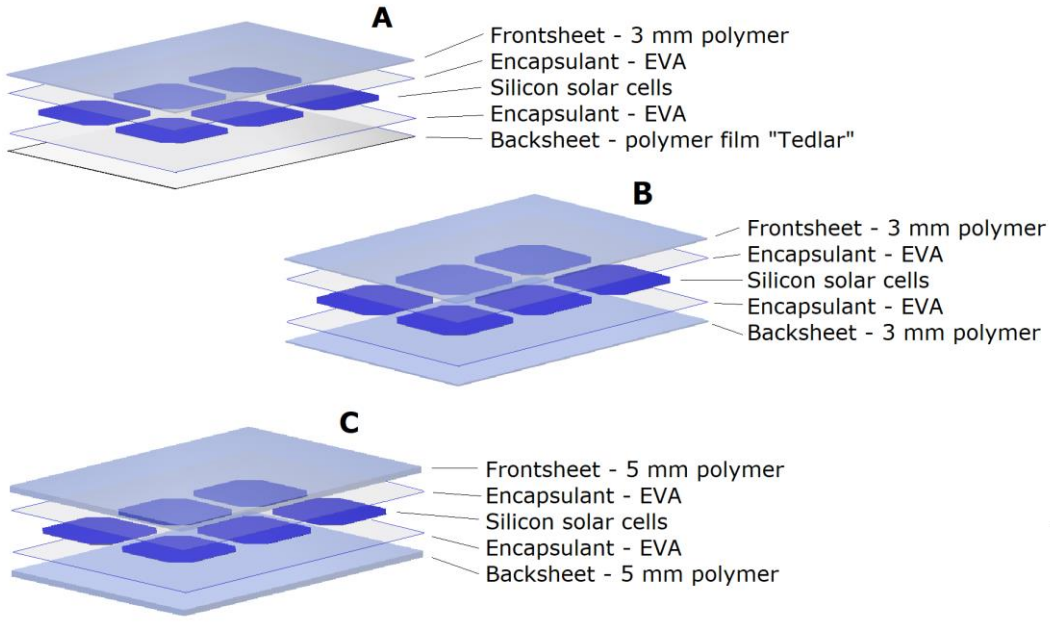

Figure 27. 3 different configurations (A, B and C) of a solar panel layers to test their effect to a post-lamination curving. (EVA – ethylene-vinyl acetate)

Curving radius and conclusion

3 laminated solar panels with different layerings are seen in **Figure 28**. Measurement of curving radius was taken according to the explanations in **Item 2.2.5**. Layering A has an asymmetrical layering, since front and backsheet are made from different materials; this solar panel has a curving radius of **1.3 m**. Symmetrical layering B with 3 mm PC on both sides reduced the curving radius to **5.0 m**. Symmetrical layering C with 5 mm PC on both sides reduced the curving radius even further – to **7.3 m**.

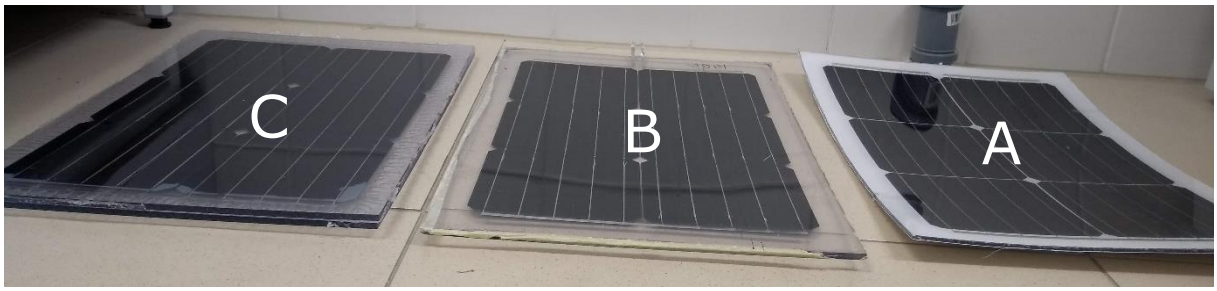

Figure 28. Laminated 3 test solar panels with different layering configurations (A, B and C) of the solar panel for the examination of post-lamination curving. Explanation of configurations on previous figure.

The curvature of all 3 solar panels was in the same direction, towards the frontsheet, and curving was visible even by visual examination. The symmetrical layering (B and C) was expected to eliminate the curving, but in fact only managed to reduce the curving as compared to layering A. As the frontsheet side of the panels was facing toward the heating elements, therefore it is expected, that frontsheet side could have experienced few degrees higher temperature and shrink more during cooling. This could have offset the balance point toward the frontsheet in turn. Layering C reduced the curving radius the most due to increased stiffness of the frontsheet and backsheet. However, this also increases the weight of the panel and reduces its flexibility. About 6 mm PC or PMMA sheet weighs as much as 3.2 mm low-iron glass, which makes 3 mm sheet thickness the limit for a symmetrical configuration panel. Instead of thick polymer, other high stiffness materials could be used as a backsheet. Commonly used alternative backsheets for semi-flexible solar panels are aluminum, stainless steel and glass-textolite. Additional propositions to reduce the curving radius are using thicker EVA, smaller cells and laminator with two-sided heating elements. Martin M. Hackmann *et al.* [24] concluded, that thicker EVA layer and smaller size of the cells would decrease the curving due to the higher relaxation. Two-sided laminator ensures uniform heating of both sides.

3.4 Testing of the adhesion between frontsheet and encapsulant

Problems and criterions associated with adhesion between solar panel frontsheet and encapsulant was discussed in **Item 1.4.5.** By changing the frontsheet material of a solar panel from low-iron glass to polymer (in this case PMMA or PC), the encapsulant glue EVA might not achieve the necessary adhesion strength. For this reason, the aims of this section are:

- Find appropriate surface treatment for PMMA and PC in order to achieve adequate adhesion with encapsulant EVA. Surface treatments were found from literature and were presented in **Item 2.1.2.** Adhesion strength between frontsheet material and encapsulant EVA was measured with peel test.
- Investigation of the frontsheet's surface to determine the prerequisites of an adequate adhesion with encapsulant EVA, which includes measuring of the surface free energy (SFE) and roughness. If one of these measurement methods are able to give reliable output on adhesion ability, then labor intensive peel test could be avoided.

3.4.1 Peel test for frontsheet-encapsulant set

Peel test is a method to directly measure the adhesion strength between solar panel frontsheet and encapsulant EVA; method itself was described in **Item 1.4.5.** According to findings of **Item 1.4.5,** the desired adhesion strength should be higher than 7.5 N/mm. This item covers the results and discussion of the peel test.

Results of peel test are seen in **Figure 29** in following classification: low-iron glass reference in group A, PMMA surface treatments in group B and PC surface treatments in group C. Low-iron glass is a reference frontsheet material, because it is used in traditional rigid solar panels and possess adequate adhesion with encapsulant EVA. Adhesion strength value of 5.8 N/mm was recorded for low-iron glass laminate, which was not as high as expected, but is still a satisfactory result according to encapsulant producer STR Holdings [60]. Results on PMMA and PC are discussed under separate bullet points:

- **Group B (PMMA):** As already noticed in prototype phase, PMMA adhesion with EVA is poor; most of the treatments were not able to improve that significantly. Gritblasting and sandpaper were able to improve the adhesion up to 2 N/mm probably due to increased surface area and mechanical interlocking. Chemicals (12M 5' and 12M 30'), flame and UV treatment were all supposed to increase the

adhesion due to increased share of functional groups on the surface. Interestingly, there was no sign of improvement for chemical and flame treatment as they lowered the adhesion value to a situation which resulted with partial delamination of the frontsheet. UV treatment however managed to achieve an excellent result of 9.8 N/mm. UV treatment could have achieved this due to chain scission of PMMA monomer. Loose ends of monomer chain can be entangled with chains of EVA.

- **Group C (PC):** Untreated PC (control) achieved a relatively high adhesion value (8.5 N/mm), exceeding the result of low-iron glass. Gritblasting and sandpaper reduced the adhesion (compared to control), which makes the theory of interlocking and increased contact area questionable. Surprisingly negative effect was noticed with UV treatment, as the sample delaminated long before the peel test. Another study on adhesion between UV treated PC and liquid silicone rubber however showed effective increase in adhesion strength due to rearrangement of the polycarbonate main chain and formation of new functional groups [83]. The measurement of surface free energy in next item does confirm new functional groups due to increased polarity, but no increase in adhesion is followed. UV treated PC surface might just not be suitable for adhesion with EVA. Chemical treatment 18M 5' had problems as well with spontaneous delamination and showed an insufficient result of 3.6 N/mm. Cr 5' and flame treatment, however, were the only ones to increase the adhesion strength above control surface. During preparation of surfaces, it was noticed that Cr 5' treatment produced completely wetting surface, which could have been an important factor in initiating adhesion.

As seen in the discussion and results of **Figure 29**, PC and PMMA acts in opposite ways to all of the treatments. For this reason, it is not possible to point out any treatment, that can universally improve the adhesion strength to encapsulant EVA.

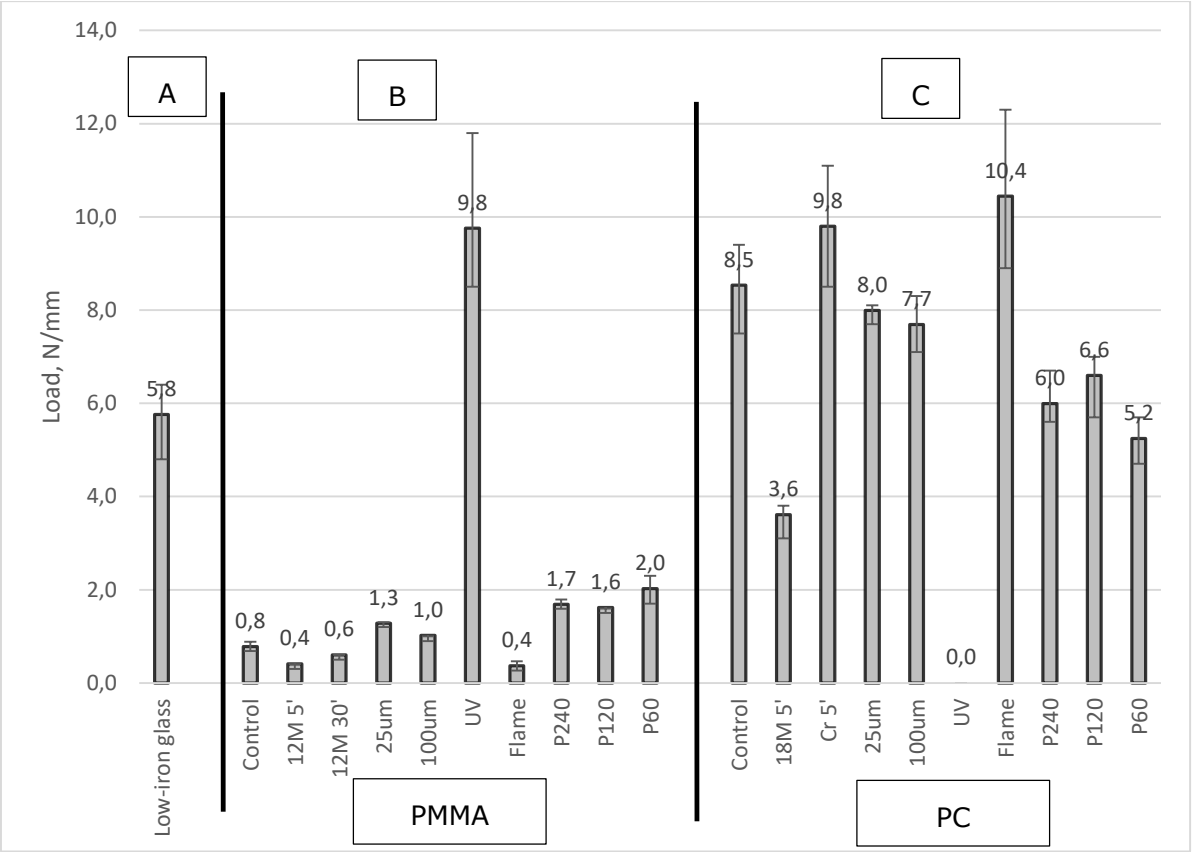

Figure 29. Peel test adhesion strength values between EVA and various surfaces. Group A (reference), group B (PMMA and its treatments), group C (PC and its treatments). **Table 2** in experimental description part further explained the abbreviations of surface treatments

3.4.1.1 Surface free energy of the frontsheet

The following tests were made in order to evaluate weather surface free energy measurement of PMMA and PC surface treatments can be considered as an indirect method for adhesion strength evaluation. Surface free energy of materials show the unrealized bonding energy of their surface. This energy can be used to describe adhesion and wetting between materials. Generally, increase in surface free energy denotes increase in wetting, which in turn is proposed to be a suitable precondition for high adhesion [69].

Current work follows the model of Owens and Wendt, by which the SFE is divided to polar and dispersive part, hence, to distinguish the necessary share of those parts, PMMA and PC surface treatments were compared with low-iron glass, as it has proved to possess adequate adhesion with encapsulant EVA. Detailed process of SFE measurement was described in **Item 2.2.2**; measurement results, discussion and comparison with peel test results are the focus points of this item.

Figure 30 presents the SFE values of frontsheet materials in 3 groups. Group A on the left represents the reference material low-iron glass. Group B in the middle represents PMMA surface treatments. Group C on the right represents PC surface treatments. Low-iron glass had a SFE value of 62 mN/m, which is similar with the values of regular window glass [84] [85]. Low-iron glass possessed a high share of polar component, which is why highly polar liquids like water wet its surface. Results of PMMA and PC surfaces are discussed under separate bullet points:

- **Group B (PMMA):** It is clearly seen that untreated PMMA (control) is a non-polar (dispersive) material, as the polar share of SFE was low. UV treatment alone managed to increase the polar component, which resulted in total SFE of 67 mN/m. With increased SFE, the surface is easily wetted, which in turn resulted in higher adhesion, as seen in previous item. As discussed in **Item 2.1.2,** UV light degrades the surface of material by chain scission, which in turn opens up possibility for the formation of additional functional groups that increase the polarity of a material surface. The other surface treatments, however, did not manage to increase surface polarity, which resulted in lower adhesion strength, as the previous item depicted. Some of the mechanically roughened surfaces (25 µm, 100 µm gritblasting and P240, P120, P60 sandpaper) resulted in polar share of almost 0 mN/m, which lead to a conclusion, that these SFE values cannot be assumed very reliable. The problem lies in contact angle measurements, as it was difficult to achieve a non-elliptical drop with the used liquids (water and diiodomethane).
- **Group C (PC):** Similarly, with PMMA, untreated PC (control) had low polar component. In this case, however, the adhesion strength to EVA was satisfactory, as seen in previous item. UV treated PC had high SFE as well due to high polar component. High polar component was also observed for chromic mixture treatment (Cr 5'), although another study have shown even higher polarity [67]. The reason behind that is too short treatment time and aging of the treated surface. Overall, both of the surfaces were indeed easily wetted by polar liquid (water). This, however, did not result with high adhesion strength for UV treated surface. Cr 5' and flame treatment achieved the highest adhesion strength in **Item 3.4.1**, however, by looking at the SFE values in **Figure 30,** high adhesion of these 2 surfaces is not very evident, because flame treatment experienced rather low polar component and overall SFE. A different result was seen on gritblasted surfaces (25 µm, 100 µm), which achieved a relatively high SFE of 52 mN/m only due to the rise of dispersive part. Increased dispersive part, however, did not result in improved adhesion strength, which can be seen in previous item.

The comparison of SFE proves that PC and PMMA do not act similarly with same surface treatments. It can be concluded that PMMA adhesion strength to EVA can be assumed by SFE measurement. For PC these parallels cannot be drawn.

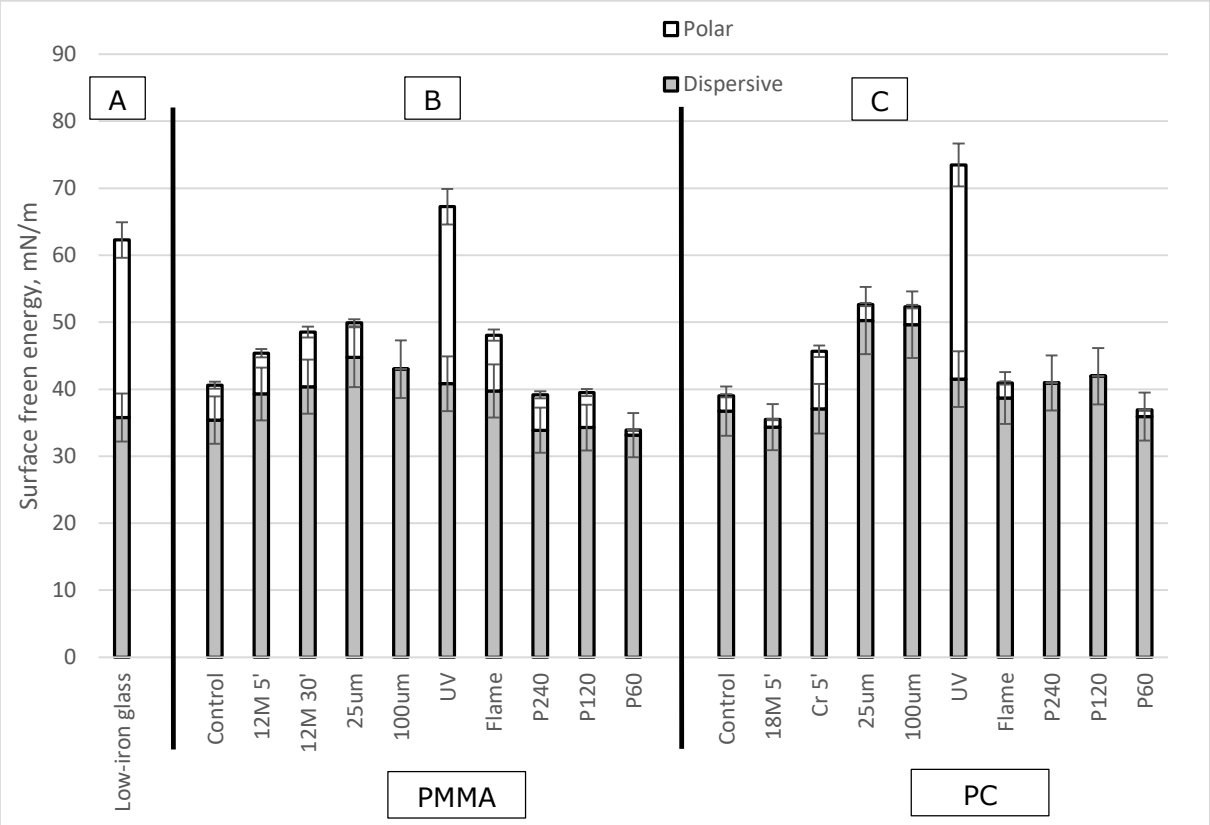

Figure 30. Surface free energy values of various surfaces. Surfaces are divided to 3 groups: group A (reference low-iron glass), group B (PMMA and its treatments), group C (PC and its treatments). Total surface free energy consists of polar part (white) and dispersive part (gray). **Table 2** in experimental description part further explained the abbreviations of surface treatments

3.4.2 Surface roughness of frontsheet

The effect of surface treatments to surface roughness was investigated, because in addition to surface free energy, mechanical interlocking can be responsible for adhesion. According to that, the purpose of this item was to examine if adhesion ability could be assumed by simple roughness measurements. Roughness was measured by profilometry and haze.

Profilometry

Profilometer scanned an area of 4,830 µm x 3,623 µm on frontsheet material and mapped surface height differences in a way to form a 3D map (**Figure 31**). For a numerical value, an arithmetic mean height of a surface (*Sa*) (hereinafter referred to as "roughness") was used and the values are presented in **Figure 32** and **Figure 33**.

Untreated PC and PMMA (control) surfaces had a roughness values of 7.9 nm and 9.3 nm, respectively. UV and flame treatment did not increase roughness of PMMA and PC surface, however, according to peel test (UV treatment of PMMA and flame treatment of PC) achieved significant increase in adhesion strength. The same correlation applied for chromic mixture treatment (Cr 5') of PC. Estimation on roughness increase for UV treated PC was proposed by [65] based on SEM pictures, which however might not be relevant for surface roughness estimation. From the correlation of surface roughness and peel strength, we can conclude that no mechanical interlocking was present for UV, flame and Cr 5' treatments, thus, roughness measurement method is not suitable in prediction of surface adhesion ability. 18M sulfuric acid (18M 5'), which was applied to PC, and 12M sulfuric acid (12M 5' and 12M 30'), which was applied to PMMA, managed to increase the surface roughness. PC's roughness increased less than for PMMA – to a roughness value of 13.9 nm due to high sulfuric acid resistance. Sulfuric acid treatment on PMMA increased the roughness to an average value of 27 nm, which, however, did not result in increase of adhesion strength as seen in peel test item. We can conclude that increase in small scale roughness (from about 8 nm to 28 nm) does not necessarily result in higher adhesion ability.

Measurement values of sandpaper and gritblasting treatments (P60, P120, P240, 100 µm, 25 µm) in **Figure 33** had to be separated from previous treatments, since roughness values of sandpaper and gritblasting are 100 times higher. P240 sandpaper with an average particle size of 58.5 µm [86] produced similar roughness as gritblasting with a particle size of 100 µm. If mechanical interlocking is most responsible for the adhesion, then peel test results of P240 and 100 µm should have been similar. Peel test adhesion strength values in **Figure 29** do not confirm that for neither PMMA nor PC. Sandpaper P60 produced the highest value of roughness (about 5200 nm) due to its large particle size of 265 µm [86], but did not result in significantly higher adhesion strength than other sandpaper or gritblasting treatments.

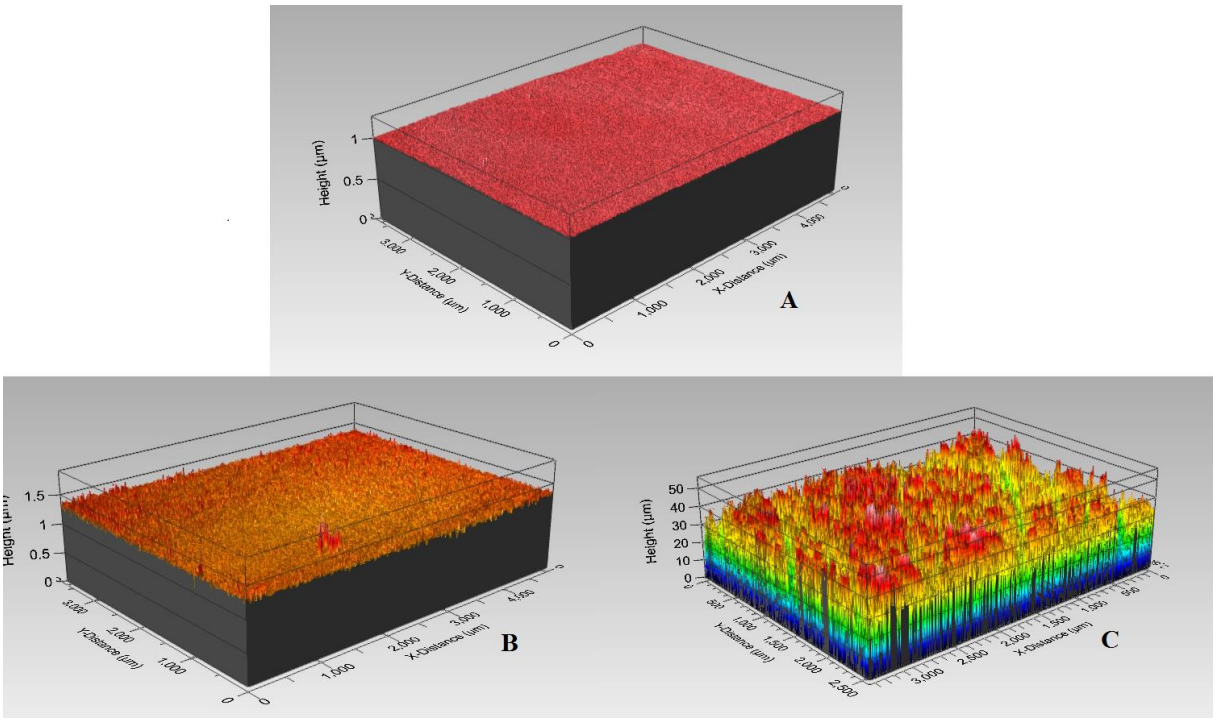

Figure 31. Examples of surface roughness 3D images. A – PMMA untreated (control), B – PMMA 5-minute sulfuric acid treatment (12M 5’), C – PMMA sandpaper treatment (P60)

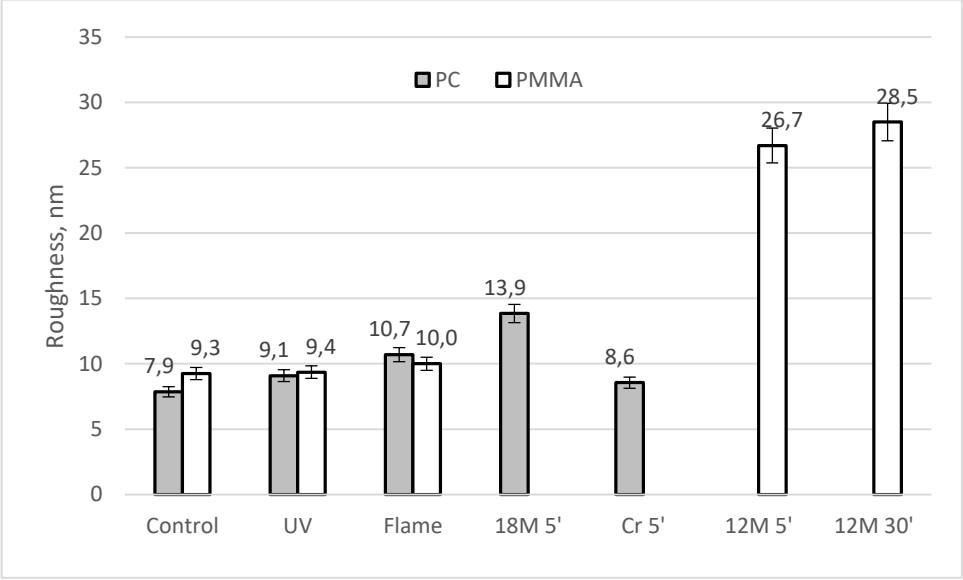

Figure 32. Small scale (up to 28.5 nm) surface roughness values of PC and PMMA surface treatments. Small scale roughness was produced by untreated (control), UV, flame, chromic mixture (Cr 5’) and sulfuric acid (18M 5’, 12M 5’ and 12M 30’). **Table 2** in experimental description part further explained the abbreviations of surface treatments. Roughness measured with arithmetic mean height of a surface (*Sa*)

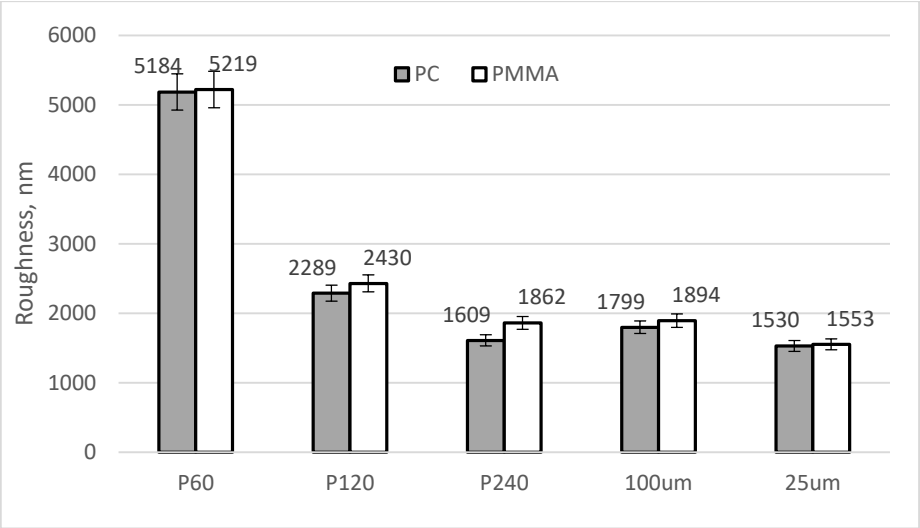

Figure 33. Large scale (up to 5219 nm) surface roughness values of PC and PMMA surface treatments. Large scale roughness was produced by sandpaper (P60, P120, P240) and gritblasting (100 µm, 25 µm). **Table 2** in experimental description part further explained the abbreviations of surface treatments. Roughness presents the arithmetic mean height of a surface (*Sa*)

Haze

Haze values of PMMA and PC after surface treatments (**Figure 34**) show light scattering of material on different wavelengths. As an addition to surface roughness, light is scattered because of porosity, crystal structure, impurities, mechanical and chemical degradation. For a more convenient comparison, average haze percentage was calculated in the range of 340 nm to 1100 nm (**Table 7**). Average haze percentage of sulfuric acid treated PMMA (12M 5', 12M 30') indicates an increase from 0.45% to 1.16% which is in correlation with results from profilometry that indicated increase in surface roughness. Increase in haze and roughness, however, did not result in significant change in peel test values, that was presented in **Figure 29**. On the other hand, UV and flame treatment on PMMA and PC did not indicate remarkable change in haze, but resulted in high values of peel test. According to previous, there seems to be no direct correlation between haze and adhesion. Mechanical surface treatments (25 µm, 100 µm, P60, P120, P240) experienced higher haze than the rest of the surface treatments, because surface of the material has been turned to translucent. This can be distinctly seen in **Figure 34,** where mechanical treatments of PMMA and PC are in the upper region of the graph. But on the contrary, higher haze did not result in higher peel test values indicating that surface irregularities and mechanical interlocking were not significantly influencing the adhesion. 25 µm gritblasting on PMMA and PC differed from other mechanical surface treatments as seen in **Figure 34** (blue and orange diagonal lines), which can be explained by the size of the scratches. Low haze value in IR region refers to lack of large scratches, because they mostly affect long IR waves. As a

conclusion, haze values of surface treatments do indicate minor relations with adhesion ability, but in overall, this method does not give reliable conclusion on adhesion ability.

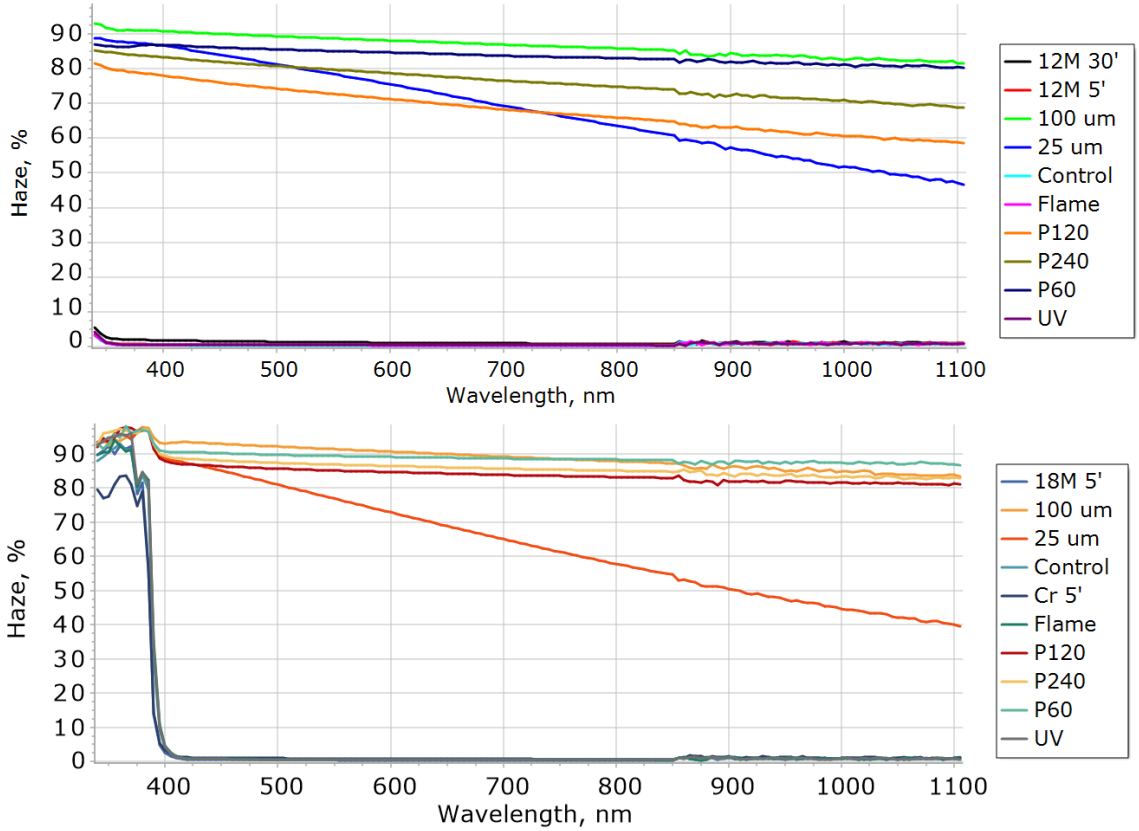

Figure 34. Haze of PMMA (upper) and PC (lower) after surface treatments give an indication on light scattering on different wavelengths. **Table 2** in experimental description part further explained the abbreviations of surface treatments

Table 7. Haze of PMMA and PC after surface treatments shows an average of haze values from wavelength 340 nm to 1100 nm. **Table 2** in experimental description part further explained the abbreviations of surface treatments

Surface treatment	PMMA haze, %	PC haze, %
Control	0.45	6.54
UV	0.55	6.78
Flame	0.52	6.63
18M 5'	-	6.18
Cr 5'	-	5.95
12M 5'	1.10	-
12M 30'	1.16	-
P60	83.65	88.96
P120	68.25	84.42
P240	76.35	86.15
100um	86.62	88.90
25um	86.62	64.52

SUMMARY

The aim of the work was to determine the feasibility of polycarbonate (PC) and polymethyl methacrylate (PMMA) in the production of semi-flexible solar panels. These polymers have a long history of outdoor environment, use but lack experience in solar cell protection. Researches and examples of PC and PMMA solar panels are rare but promising, as the literature shows suitable properties for solar panel use.

Literature overview has concluded semi-flexible panels to be a niche product for specific purposes like marine sector, portable device sector, etc. Main problems of the polymers are poor adhesion, high thermal expansion, high water and oxygen transmission rate. Poor adhesion of the polymers can be modified by multiple surface treatments. However, unambiguous mechanism behind a good adhesion is yet unknown. Low stiffness and high thermal expansion of polymer frontsheets are responsible for post-lamination curving of the solar panel. After the 140 °C lamination, the decreasing temperature of the panel induces stress between different layers and result in curving. Options to relieve curving are using a thicker layer of EVA or smaller size of solar cells, which provide higher degree of stress relaxation. Thicker layer of frontsheet reduces curving due to higher stiffness.

Experimental section concluded the work objectives as follows:

1. According to properties found in literature, PC and PMMA can offer various advantages over other solar panel cover materials. Current polymers are price-competitive, lightweight and resistant to mechanical impact. PMMA is a material with particularly high transmittance (92%), whereas PC transmittance range in 88%.
2. Preliminary testing showed very poor adhesion of commercial untreated PMMA with EVA, but no signs of delamination for PC. Electrical measurements of prototype solar panels showed 1,6% and 2,9% lower cell efficiency for PMMA and PC solar panel than for low-iron glass solar panel. Lower value could come from high UV cut-off wavelength of PMMA and PC at ~400 nm. High thermal expansion of PC and PMMA caused post-lamination curving of the solar panel. Symmetrical configuration of a solar panel with PC on both outer sides increased the curving radius from 1,3 m to 5 m; higher thickness of sheets can increase it further but affects the flexibility of the solar panel. Results are still far from satisfyingly flat panel.
3. Gritblasting, sandpaper, UV, chemical and flame treatment were used on PC and PMMA frontsheet to increase the adhesion with EVA encapsulant. Peel test

indicated sufficient adhesion strength for UV treated PMMA, untreated PC, chromic mixture etch PC, flame treated PC and gritblasted PC. Investigation of surfaces included measurement of surface free energy and roughness to determine the prerequisites of a good adhesion with EVA. Surface free energy measurement can determine the increase of polar component, which strongly affect the adhesion strength of PMMA. PC adhesion ability is not easily determined as it does not behave similarly to PMMA. Overall, surface free energy and roughness do not produce reliable and consistent connection with peel test adhesion strength.

According to this work, PMMA seems to be more prospective as a frontsheet of a semi-flexible solar panel. Further testing could be done on solvent and ultrasonic welding of front- and backsheets. These techniques have a potential for a strong adhesion and would eliminate the problem of thermal expansion. Environmental test for moisture and temperature fluctuation from - 40 $^{\circ}$C to 85 $^{\circ}$C would be a necessary next step for the feasibility evaluation.

LIST OF REFERENCES

[1] J. Tsao, N. Lewis and G. Crabtree, "Solar FAQs," 2006.

[2] Fraunhofer Institute for Solar Energy Systems, "PHOTOVOLTAICS REPORT," Freiburg, 2019.

[3] M. Mazzucato and G. Semieniuk, "Financing renewable energy: Who is financing what and why it matters," *Technological Forecasting and Social Change,* vol. 127, pp. 8-22, February 2018.

[4] Images SI Inc., "Photovoltaic Cells – Generating electricity," 20 April 2020. [Online]. Available: https://www.imagesco.com/articles/photovoltaic/photovoltaic-pg4.html.

[5] A. Hussain, "F.Sc ICS Notes: Physics XII: Chapter 17," 17 February 2015. [Online]. Available: https://fscnotes0.blogspot.com/2015/02/fsc-ics-notes-physics-xii-chapter-17-physics-of-solids-exercise-short-questions.html.

[6] Tindo Solar, "Types of Crystalline silicon cells," 25 April 2020. [Online]. Available: https://www.tindosolar.com.au/learn-more/poly-vs-mono-crystalline/.

[7] Beijing Epsolar Technology Co., Ltd, "How solar panels are built?," 23 September 2019. [Online]. Available: https://blog.epsolarpv.com/articles/12/how-solar-panels-are-built-.

[8] NREL, "Best Research-Cell Efficiency Chart," 21 May 2019. [Online]. Available: https://www.nrel.gov/pv/cell-efficiency.html.

[9] L. Youn-Jung, K. Yung-Sun and S. M. Ifitiquar, "Silicon Solar Cells: Past, Present and the Future," *Journal of the Korean Physical Society,* pp. 355-261, 2014.

[10] R. Dunbar, "How Efficient Will Solar PV Be In The Future? 10-Year Predictions For The Industry," 15 August 2017. [Online]. Available: https://cleantechnica.com/2017/08/15/efficient-will-solar-pv-future-10-year-predictions-industry/.

[11] SunPower, 19 May 2019. [Online]. Available: https://us.sunpower.com/solar-resources/sunpower%C2%AE-x-series-residential-dc-x22-370.

[12] LG Electronics, 20 May 2019. [Online]. Available: https://www.lg.com/us/business/solar-panel/all-products/lg-LG360Q1C-A5.

[13] Eesti Energia, "Päikesepaneelide kalkulaator," [Online]. Available: https://www.energia.ee/et/era/taastuvenergia/paikesepaneelid. [Accessed 14 May 2020].

[14] Smartecon, "Päikesepaneelide hinnad," [Online]. Available: https://smartecon.ee/paikesepaneelide-hinnad/. [Accessed 14 May 2020].

[15] R. Fu, D. Feldman and R. Margolis, "U.S. Solar Photovoltaic System Cost Benchmark: Q1 2018," October 2018. [Online]. Available: https://www.nrel.gov/docs/fy19osti/72133.pdf.

[16] K. Sopian, S. Cheow and S. Zaidi, "An overview of crystalline silicon solar celltechnology: Past, present, and future," in *AIP Conference Proceedings*, 2017.

[17] ENF Solar, "Monocrystalline - Solar Panel Manufacturers," 13 April 2020. [Online]. Available: https://www.enfsolar.com/directory/panel/monocrystalline.

[18] M. Valner, "Eesti taastuvenergia arengukavas napib ambitsiooni," 1 October 2019. [Online]. Available: https://www.aripaev.ee/raadio/episood/eesti-taastuvenergia-arengukavas-napib-ambitsiooni.

[19] Orian Research, "Global Flexible Solar Panels Market Research Report 2019," 15 February 2019. [Online]. Available: https://www.orianresearch.com/report/flexible-solar-panels/804264.

[20] Eco Industrial Supplies, "Solar Panels Flexible," 9 October 2019. [Online]. Available: https://www.ecoindustrialsupplies.com/solar-panels-flexible-bendable.html.

[21] E. Gruber, "R & D Work on the Encapsulation of Solar Cells with Improved Potting and Cover Materials," in *Photovoltaic Power Generation*, Brussels, 1982.

[22] Emerald Group Publishing Limited, "Polymers in solar modules," *Pigment & Resin Technology,* vol. 40, no. 1, 2011.

[23] D. Losado, "Technology for sustainable future," 29 April 2017. [Online]. Available: https://crecimiento-sostenible.blogspot.com/2017/04/building-photovoltaic-solar-panel-using.html#more.

[24] M. M. Hackmann, M. H. H. Meuwissen, T. L. Bots, J. A. H. M. Buijs, K. M. Broek, R. Kinderman, O. B. F. Tanck and F. M. Schuurmans, "Technical feasibility study on polycarbonate," *Solar Energy Materials & Solar Cells,* pp. 105-115, 2004.

[25] AZoBuild, "Polycarbonate Encapsulated Solar Cells - News Item," Febuary 2002. [Online]. Available: https://www.azobuild.com/article.aspx?ArticleID=1386.

[26] Galaxy Energy GmbH, "PC Modul – Kinderleicht montieren," 9 May 2020. [Online]. Available: http://www.galaxy-energy.com/en/project/pc-modul/.

[27] J. Zhou, J. Pickett, S. Davis, S. Chakravarti and . M. J. Davis, "IMPROVED RELIABILITY OF PV MODULES WITH LEXAN™ (PC) SHEET - FRONT SHEET," February 2013. [Online]. Available: https://www.energy.gov/sites/prod/files/2014/01/f7/pvmrw13_ps5_sabic_zhou.pdf.

[28] E. Gorgan, "Energy Observer Catamaran Crosses the Atlantic With Zero Emissions, High Comfort," 12 May 2020. [Online]. Available: https://www.autoevolution.com/news/energy-observer-catamaran-crosses-the-atlantic-with-zero-emissions-high-comfort-143543.html.

[29] Solbian, "Solbian SolarExpo," 7 October 2012. [Online]. Available: https://www.solbian.eu/en/blog/solbian-solarexpo-n164.

[30] DuPont, "DuPont Frontsheet Materials," 27 April 2015. [Online]. Available: https://www.chemours.com/Teflon_Industrial/en_US/assets/downloads/k23269_Teflon_films.pdf.

[31] S. Black, "Simplifying the solar panel with composites," 13 November 2017. [Online]. Available: https://www.compositesworld.com/articles/simplifying-the-solar-panel-with-composites-.

[32] AI Technology, Inc, "SOLAR-THRU™: A Single Ply Fluorinated Melt-Encapsulating PVDF Front Sheet For Instant Melt-Bonding Lamination," 20 August 2019. [Online]. Available: https://www.aitechnology.com/products/solar/transparent-pvdf-encapsulating-front-sheet/.

[33] Renewable Energy World, "Three options for "good enough" solar module frontsheets," 15 June 2011. [Online]. Available: https://www.renewableenergyworld.com/2011/06/15/three-options-for/#gref.

[34] Plastics Technology, "Looking into Photovoltaic Film? Here Are Material & Die-Design Insights," 28 January 2012. [Online]. Available: https://www.ptonline.com/articles/looking-into-photovoltaic-film-here-are-material-die-design-insights.

[35] DuPont Teijin Films., "Polyester Films for Front Sheet Substrate Applications," 18 October 2019. [Online]. Available: https://usa.dupontteijinfilms.com/markets-and-applications/photovoltaics/front-sheet-materials/.

[36] Qookka, "ETFE and PET: Two key materials in the field of semi-flexible panels," 5 August 2017. [Online]. Available: https://www.qookka.com/en/blog/etfe-and-pet-two-key-materials-in-the-field-of-semi-flexible-panels-n3.

[37] G2V Optics Inc., "Solar simulation," 31 March 2020. [Online]. Available: https://g2voptics.com/solar-simulation/.

[38] C. Deziel, "The Effect of Wavelength on Photovoltaic Cells," 1 December 2018. [Online]. Available: https://sciencing.com/effect-wavelength-photovoltaic-cells-6957.html.

[39] T. F. El-Shater and M. Rienäcker, "Why is that the best band gap of a solar cell is in the region of 1.5 eV?," December 2014. [Online]. Available: https://www.researchgate.net/post/Why_is_that_the_best_band_gap_of_a_solar_cell_is_in_the_region_of_15_eV.

[40] Saint-Gobain, "SGG DIAMANT," 19 February 2018. [Online]. Available: https://uk.saint-gobain-building-glass.com/en-gb/sgg-diamant.

[41] J. Pern, "Module Encapsulation Materials, Processing and Testing," 4 December 2008. [Online]. Available: https://www.nrel.gov/docs/fy09osti/44666.pdf.

[42] P. Hülsmann, K. Weiß and M. Köhl, "Temperature-dependent water vapour and oxygen permeation through different polymeric materials used in photovoltaic-modules," *Progress in photovoltaics,* pp. 415-421, 2012.

[43] J. A. Hauch, P. Schilinsky, S. A. Choulis, S. Rajoelson and C. J. Brabec, "The impact of water vapor transmission rate on the lifetime of flexible polymer solar cells," *Applied Physics Letters,* vol. 93, no. 10, 9 September 2008.

[44] C. Lungenschmied, G. Dennler, G. Czeremuszkin, M. Eche, H. Neugebauer and N. S. Sariciftci, "Flexible encapsulation for organic solar cells," *Proceedings of SPIE - The International Society for Optical Engineering,* vol. 6197, 2006.

[45] Omnexus, "Haze; Transparency; What is PVDF?; Water Absorption 24 hours; Max Continuous Service Temperature; Coefficient of Linear Thermal Expansion," 24 February 2020. [Online]. Available: https://omnexus.specialchem.com/.

[46] U. Eitner, S. Kajari-Schröder, M. Köntges and H. Altenbach, "Thermal Stress and Strain of Solar Cellsin Photovoltaic Modules," in *Shell-like structures*, Berlin, Springer, 2011, pp. 453-468.

[47] F. M. Ashby, Materials and the Environment (Second Edition), Elsevier, 2013, pp. 459-595.

[48] Abrisa Technologies, "Soda-lime low-iron," January 2014. [Online]. Available: https://abrisatechnologies.com/products-services/glass-products/soda-lime-glass/low-iron/.

[49] P. Becker, P. Scyfried and H. Z. Siegert, "The Lattice Parameter of Highly Pure Silicon Single Crystals," *Physik B - Condensed Matter,* p. 17–21, 1982.

[50] Engineering ToolBox, "Coefficients of Linear Thermal Expansion," 10 May 2019. [Online]. Available: https://www.engineeringtoolbox.com/linear-expansion-coefficients-d_95.html.

[51] L. Yixian and A. A. O. Tay, "FINITE ELEMENT THERMAL STRESS ANALYSIS OF A," National University of Singapore, Singapore, 2011.

[52] M. C. C. Oliveira, A. S. A. D. Cardoso, M. M. Viana and V. F. C. Lins, "The causes and effects of degradation of encapsulant ethylene vinyl acetate copolymer (EVA) in crystalline silicon photovoltaic modules: A review," Elsevier, 2017.

[53] S. Krauter, R. Penidon, B. Lippke, M. Hanusch and P. Grunow, "PV module lamination durability," in *ISES Solar World Congress*, Berlin, 2011.

[54] F. Awaja, M. Gilbert, G. Kelly, B. Fox and P. J. Pigram, "Adhesion of polymers," *Progress in Polymer Science,* vol. 34, no. 9, p. 948–968, 2009.

[55] H. Peets, "Eesti vabaõhumuuseum," 22 November 2005. [Online]. Available: https://evm.ee/uploads/files/loeng09.pdf.

[56] Polymer Properties Database, "Adhesion of Polymers," 23 May 2018. [Online]. Available: https://polymerdatabase.com/polymer%20physics/Adhesion.html.

[57] S. Ebnesajjad, Surface Treatment of Materials for Adhesive Bonding, William Andrew, 2014, pp. 3-77, 197-202.

[58] F. J. Pern and S. H. Glick, "Adhesion Strength Study of EVA Encapsulants on Glass Substrates," in *National Center for Photovoltaics and Solar Program Review Meeting*, Colorado, 2003.

[59] E. Wang, H. E. Yang, K.-H. Yen and C. Wang, "Reliability and safety study of polymeric materials used in photovoltaic modules," in *The 21rd International Photovoltaic Science and Engineering*, Fukuoka, 2011.

[60] Specialized Technology Resources, Inc., "Test methods," 29 February 2020. [Online]. Available: http://www.strsolar.com/test-methods/.

[61] K. Drabczyk, "Study of lamination quality of solar modules," *Microelectronics International,* pp. 100-103, 2019.

[62] Nantong Reoo Technology Co., Ltd, "Products," 10 April 2020. [Online]. Available: http://www.reoo.net/en/products.html.

[63] A. G. G. Toh, Z. F. Wang and S. H. Ng, "Fabrication of Embedded Microvalve on PMMA Microfluidic Devices through Surface Functionalization," in *DTIP*, Nice, 2008.

[64] X. Zhang, Y. Zhong, X. Zhang, L. Li and Y. Yan, "Plasma and chromic acid treatments of polycarbonate surface to improve coating–substrate adhesion," *SIA,* pp. 1893-1898, 2013.

[65] T.-H. Kim, B.-S. Hwang, H.-Y. Kang, J.-H. Kim, L. D. Tijing, C. S. Kim and J. K. Lim, "Enhanced wetting and adhesion of polycarbonate by ultraviolet light surface treatment," *Digest,* pp. 1415-1421, 2013.

[66] Arcotec GmbH, "Frequently Asked Questions," 16 December 2019. [Online]. Available: http://www.arcotec.com/en/FAQ.htm.

[67] N. Taghavinia, H. Yaghoubi and E. K. Alamdari, "Self cleaning TiO2 coating on polycarbonate: Surface treatment, photocatalytic and nanomechanical properties," *Surface and Coatings Technology,* vol. 204, no. 9-10, pp. 1562-1568, 25 January 2010.

[68] L. Pandiscia, "Haze Measurement using a UV-Visible Spectrophotometer," 29 February 2020. [Online]. Available: https://jascoinc.com/applications/haze-measurement-uvvisible-spectrophotometer/.

[69] E. Spooner, "A Guide to Surface Energy," 30 April 2020. [Online]. Available: https://www.ossila.com/pages/a-guide-to-surface-energy.

[70] C. Vicente, P. André and R. Ferreira, "Simple measurement of surface free energy using a web cam," *Revista Brasileira de Ensino de Física,* 2012.

[71] Krüss, "So You Want to Measure Surface Energy?," 26 July 2017. [Online]. Available: https://www.kruss-scientific.com/fileadmin/user_upload/website/literature/kruss-tn306-en.pdf.

[72] Krüss, "Surface free energy (SFE)," 27 February 2020. [Online]. Available: https://www.kruss-scientific.com/services/education-theory/glossary/surface-free-energy/.

[73] Keyence, "Area Roughness Parameters," 16 February 2020. [Online]. Available: https://www.keyence.com/ss/products/microscope/roughness/surface/parameters.jsp.

[74] Estonian Centre for Standardisation, *EVS-EN ISO 8510-2:2010 Adhesives - Peel test for a flexible-bonded-to-rigid test specimen assembly - Part 2: 180 degree peel,* 2010.

[75] Tesa SE, "What's the deal with peel (peel adhesion, that is)?," 15 September 2016. [Online]. Available: https://www.tesa.com/en-us/wikitapia/peel-adhesion.html.

[76] Crylux, "Crylux product guide," 2017.

[77] Koscon Industrial S.A., "Macrolux® Solid XL - 3.0 mm," 2014. [Online]. Available: http://www.macroluxusa.com/macrolux-solid.

[78] The Chemours Company, "Tefzel™ ETFE," 18 October 2017. [Online]. Available: https://www.chemours.com/Teflon_Industrial/en_US/assets/downloads/tefzel-etfe-film-properties.pdf.

[79] TJ Green Associates, LLC, "Hermetic vs "Near Hermetic" Packaging A Technical Review," 28 May 2018. [Online]. Available: https://www.tjgreenllc.com/2016/09/21/hermetic-vs-near-hermetic-packaging-a-technical-review/.

[80] Thermoscientific, "Physical Properties Table," 23 August 2013. [Online]. Available: https://static.thermoscientific.com/images/D20826~.pdf.

[81] Astenik Solar (Canada) Inc., "EVA films," August 2010. [Online]. Available: http://www.asteniksolar.com/products/materials/First_eva/Product_sheet_eva.pdf.

[82] S. Ebnesajjad, Fluoroplastics, Volume 2: Melt Processible Fluoroplastics, William Andrew, 2002, p. 10.

[83] M. Hartung, M. Nikousaleh, A. Rüppel, R.-U. Giesen and H.-P. Heim, "UV Surface Treatment of Polycarbonate for Adhesion Improvement to Liquid Silicone Rubber (LSR)," *Journal of Plastics Technology,* pp. 189-209, February 2019.

[84] S. K. Rhee, "Surface energies o f silicate glasses calculated from their wettability data," *Journal of Materials Science,* vol. 12, no. 4, p. 823–824, April 1977.

[85] K. T. Tan, C. C. White, D. L. Hunston, C. Clerici, K. L. Steffens, J. Goldman and B. D. Vogt, "Fundamentals of Adhesion Failure for a Model Adhesive (PMMA/Glass) Joint in Humid Environments," *The Journal of Adhesion,* vol. 84, no. 4, pp. 339-367, April 2008.

[86] M. Bumiller, "Particle Characterization of Abrasives," 2010.

[87] G. Oreski, "Degradation of materials in PV modules," International Energy Agency, 2019.